

AD-A061 262

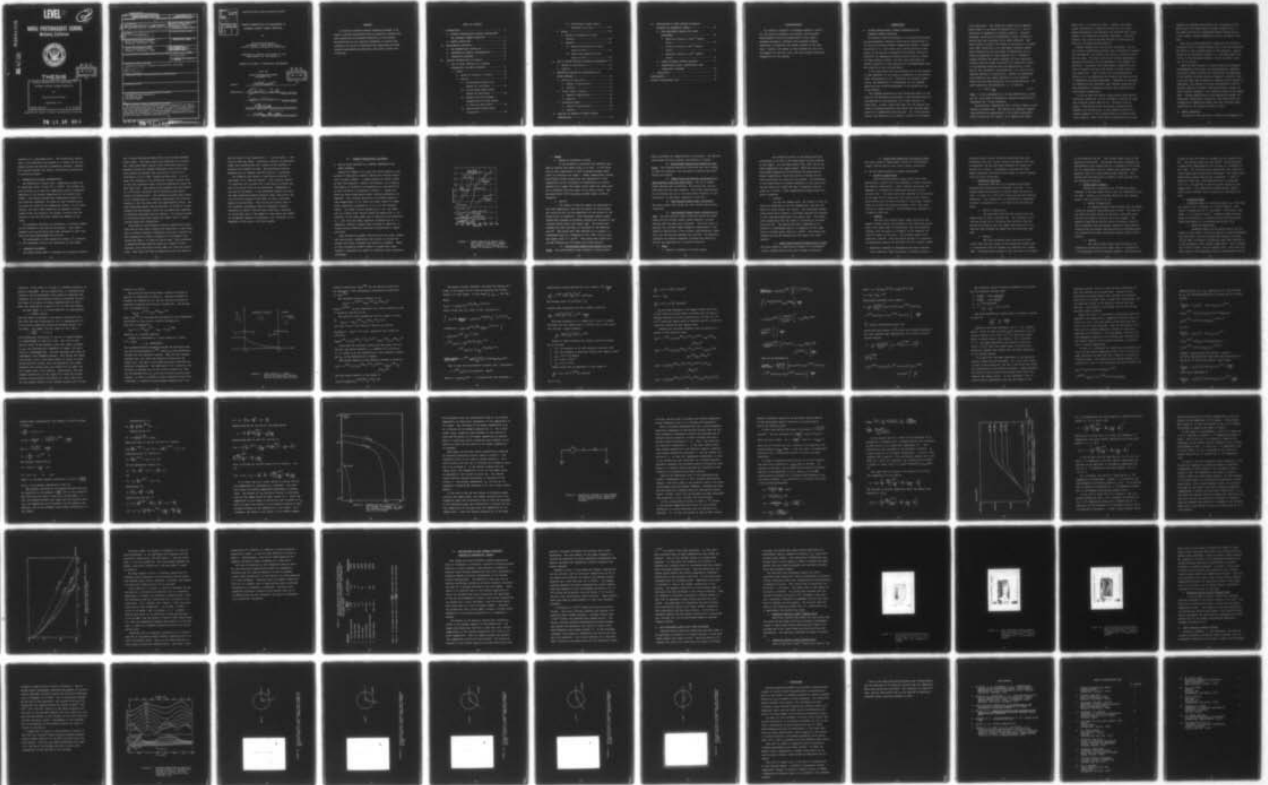
NAVAL POSTGRADUATE SCHOOL MONTEREY CALIF
SURFACE PREPARATIONS FOR ENHANCEMENT OF INFRARED SURFACE CURREN--ETC(U)
SEP 78 W D RUSSELL

F/G 17/5
NL

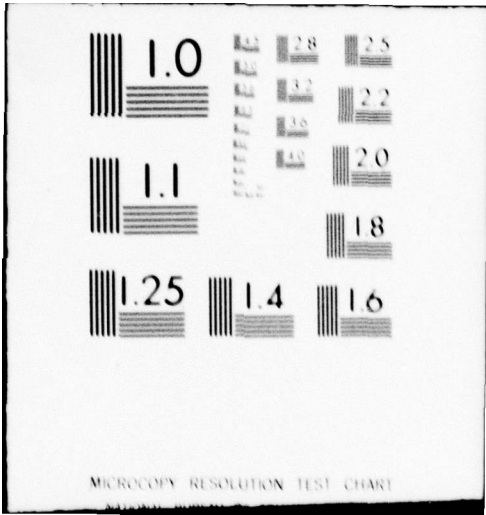
UNCLASSIFIED

NL

| of |
AD
A061 262



END
DATE
FILMED
1-79
DDC



MICROCOPY RESOLUTION TEST CHART

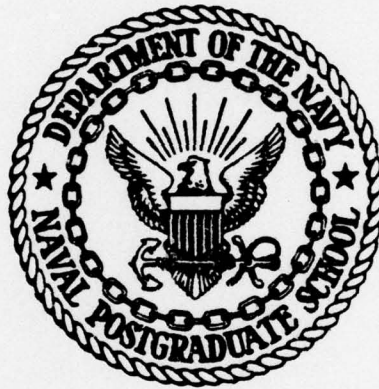
LEVEL II

2
NW

AD A061262

NAVAL POSTGRADUATE SCHOOL
Monterey, California

DDC FILE COPY



DDC
RECEIVED
NOV 17 1978
D

THESIS

SURFACE PREPARATIONS FOR ENHANCEMENT OF
INFRARED SURFACE CURRENT DETECTION

by

William David Russell

September 1978

Thesis Advisor: R. W. Burton

Approved for public release; distribution unlimited.

78 11 13 093

UNCLASSIFIED

SECURITY CLASSIFICATION OF THIS PAGE (When Data Entered)

REPORT DOCUMENTATION PAGE		READ INSTRUCTIONS BEFORE COMPLETING FORM
1. REPORT NUMBER	2. GOVT ACCESSION NO.	3. RECIPIENT'S CATALOG NUMBER
4. TITLE (and Subtitle) ⑥ SURFACE PREPARATIONS FOR ENHANCEMENT OF INFRARED SURFACE CURRENT DETECTION		5. TYPE OF REPORT & PERIOD COVERED ⑦ Master's Thesis September 1978
7. AUTHOR(s) ⑩ William David/Russell		6. PERFORMING ORG. REPORT NUMBER
9. PERFORMING ORGANIZATION NAME AND ADDRESS Naval Postgraduate School Monterey, California 93940		8. CONTRACT OR GRANT NUMBER(s)
11. CONTROLLING OFFICE NAME AND ADDRESS Naval Postgraduate School Monterey, California 93940		10. PROGRAM ELEMENT, PROJECT, TASK AREA & WORK UNIT NUMBERS
14. MONITORING AGENCY NAME & ADDRESS (if different from Controlling Office)		12. REPORT DATE ⑪ September 1978
		13. NUMBER OF PAGES 81
		15. SECURITY CLASS. (of this report) Unclassified
		15a. DECLASSIFICATION/DOWNGRADING SCHEDULE
16. DISTRIBUTION STATEMENT (of this Report) Approved for public release; distribution unlimited. ⑫ 82 p.		
17. DISTRIBUTION STATEMENT (of the abstract entered in Block 20, if different from Report)		
18. SUPPLEMENTARY NOTES		
19. KEY WORDS (Continue on reverse side if necessary and identify by block number) Infrared Current Detection AGA Thermovision Infrared Camera		
20. ABSTRACT (Continue on reverse side if necessary and identify by block number) In order for infrared current detection methods to be useful, surface preparations must be applied to enhance the heat generation and infrared emissivity of the surface. The derivation of the required parameters of surface preparations for metals is presented and comparisons are made between experimentally determined and actual current distributions.		

DD FORM 1473
1 JAN 73

EDITION OF 1 NOV 65 IS OBSOLETE
3/8 10 24-6401

UNCLASSIFIED

SECURITY CLASSIFICATION OF THIS PAGE (When Data Entered)

78 11 13 08
251 450

alt

ACCESSION NO.		
DTIC	Write Section	<input checked="" type="checkbox"/>
DDC	Diff Section	<input type="checkbox"/>
UNANNOUNCED		<input type="checkbox"/>
JUSTIFICATION		
BY		
DISTRIBUTION/AVAILABILITY STATEMENT		
Class.	AVAIL. CODE/ST	SPECIAL
A		

Approved for public release; distribution unlimited

SURFACE PREPARATIONS FOR ENHANCEMENT OF
INFRARED SURFACE CURRENT DETECTION

by

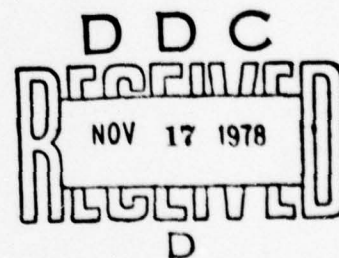
William David Russell
Lieutenant, United States Navy
B.E.E., Georgia Institute of Technology

Submitted in partial fulfillment of the
requirements for the degree of

MASTER OF SCIENCE IN ELECTRICAL ENGINEERING

from the

NAVAL POSTGRADUATE SCHOOL
September 1978



Author:

W D Russell

Approved by:

Robert W. Burton Thesis Advisor

John D. Power Second Reader

W E Kula
Chairman, Department of Electrical Engineering

William M. Latta
Dean of Science and Engineering

ABSTRACT

In order for infrared current detection methods to be useful, surface preparations must be applied to enhance the heat generation and infrared emissivity of the surface. The derivation of the required parameters of surface preparations for metals is presented and comparisons are made between experimentally determined and actual current distributions.

TABLE OF CONTENTS

I. INTRODUCTION - - - - - 8

 A. FACTORS NECESSITATING SURFACE PREPARATIONS
 FOR INFRARED CURRENT DETECTION - - - - - 8

 B. THESIS OBJECTIVES- - - - - 11

II. EXPERIMENTAL APPARATUS - - - - - 13

 A. AGA THERMOVISION SYSTEM 680- - - - - 13

 B. THERMOVISION DISPLAY INTERPRETATION- - - - - 14

 C. LABORATORY APPARATUS - - - - - 14

III. SURFACE PREPARATIONS FOR METALS- - - - - 17

 A. USE OF OXIDE COATINGS AS A SURFACE
 PREPARATION FOR METAL SURFACES - - - - - 17

 1. Copper - - - - - 19

 a. Method of Formation of Oxide - - - - - 19

 b. Results- - - - - 19

 (1) Pre-polished Copper Plate
 Heated for Five Hours - - - - - 19

 (2) Pre-polished Copper Plate
 Heated for Nine Hours - - - - - 20

 (3) Copper Plate with Natural
 Accumulation of Oxide Heated
 In Oven for Three Hours - - - - - 20

 (4) Sand Blasted Copper Sheet,
 Unoxidized- - - - - 20

(5) Sand Blasted Copper Sheet,	
Oxidized In An Oven - - - - -	20
2. Brass- - - - -	20
a. Method of Formation of Oxide	
Coating- - - - -	20
b. Results- - - - -	21
(1) Brass Plate Heated for Three	
Hours In Oven - - - - -	21
(2) Brass Plate Heated for Six	
Hours In Oven - - - - -	22
B. USE OF COPPER SULFIDE AS SURFACE PREPARATION	22
1. Method of Application- - - - -	22
2. Results- - - - -	22
C. RESISTIVE COATINGS AS PREPARATIONS FOR	
METAL SURFACES - - - - -	22
1. Television Tube Coat - - - - -	23
a. Method of Application- - - - -	23
b. Results- - - - -	23
2. Carbon (Soot) Coating- - - - -	24
a. Method of Application- - - - -	24
b. Results- - - - -	24
3. Teledeltos Paper - - - - -	25
a. Method of Application- - - - -	25
b. Results- - - - -	26
D. ANALYSIS OF RESULTS OF METAL SURFACE	
PREPARATIONS - - - - -	26

IV. APPLICATIONS TO MORE COMPLEX SCATTERING	
SURFACES OF NONMETALLIC MODELS - - - - -	60
A. HALF WAVELENGTH SQUARE FLAT PLATE	
SCATTERERS - - - - -	62
1. Resistive Coating 6.18×10^{-5} Meters	
Thick- - - - -	63
2. Resistive Coating 9.6×10^{-5} Meters	
Thick- - - - -	63
3. Resistive Coating 2.7×10^{-5} Meters	
Thick- - - - -	67
B. OTHER AVAILABLE SURFACE COATINGS - - - - -	67
C. ELECTRICALLY THICK, ELECTRICALLY LONG	
CONDUCTING CYLINDERS - - - - -	68
V. CONCLUSIONS- - - - -	77
BIBLIOGRAPHY - - - - -	79
INITIAL DISTRIBUTION LIST- - - - -	80

ACKNOWLEDGEMENT

The author is grateful to Professor Robert W. Burton for the skillful guidance, his counsel, and continual encouragement during the preparation of this report. Professor Matthew D. Kelleher also provided valuable assistance in examining the thermal aspects of this problem. Finally, the author is very grateful for the love and support of his wife, Dian, and the children during the preparation of this thesis.

I. INTRODUCTION

A. FACTORS NECESSITATING SURFACE PREPARATIONS FOR INFRARED CURRENT DETECTION

The surface currents developed in a scattering structure by electromagnetic radiation cause heating proportional to I^2R and this heating produces temperature changes. LaVarre and Burton [1], have shown that infrared detection techniques can be applied to determine the surface current by detecting the temperature profiles which arise as a result of these surface currents, and have also described the drastic reduction in time required for the measurements that was achieved by the infrared method.

It has been shown that the applicability of this process is very dependent on the physical properties of the surface under investigation [2]. Electrical and thermal conductivity, the emissivity of the material in the infrared region and the relative smoothness of the surface are critical factors.

The infrared emissivity of the scattering object is the ratio of the emittance of the body in the infrared region of the spectrum to the emittance of an ideal radiator, or black body. It has a value less than one; the greater the value of infrared emissivity the better the infrared detectability of temperature distributions. As a first approximation, the emissivity of a surface is equal to the absorp-

tion coefficient. The reflection coefficient is approximately equal to one minus the emissivity [3]. The reflectivity is dependent on surface condition. Relative roughness, oxidation and contamination cause a surface to deviate from the conditions of an ideal reflector. Adequate theory to predict the effect of deviation of a surface from ideal conditions is not developed; therefore experimental methods are the only means of determining the reflective properties of real surfaces [4]. Generally, rougher surfaces and darker surfaces are less reflective. Surfaces that are highly reflective in a particular region of the spectrum therefore have low emissivities in that region; and conversely, high emissivity in a region of the spectrum implies low reflectivity. Metals are substances which generally are highly reflective in the infrared region and are characterized by very low emissivities. For good conductors, the emissivity, ϵ_λ , is given by

$$\epsilon_\lambda = .365 \times \frac{1}{\sqrt{\sigma\lambda}} \quad [5]$$

where λ is the wavelength and σ is the conductivity in mhos per cm. This shows an emissivity inversely proportional to wavelength for a given conductor.

The electrical conductivity has a critical impact on the detection process also. The heating and resultant temperature profiles are proportional to the energy dissipation, which is given by J^2/σ where J is in amperes per square

meter, and σ is in mhos per meter. Clearly, for large values of electrical conductivity there will be little energy dissipated in the material and therefore very little heating to be detected by infrared techniques. Poor conductors, then, seem to be more suitable as scattering objects for infrared current detection.

Thermal conductivity also must be considered. As surface current distributions produce heat distributions throughout the material, the surface will tend to uniformly distribute the heat. The rate at which the heating approaches a uniform distribution will be dependent on the thermal conductivity. A material with high thermal conductivity will tend to transfer the heat from warmer to cooler areas at a very rapid rate. Thus the heat will be distributed as quickly as it is produced by the currents and there will be no temperature profiles detectable. Therefore for purposes of infrared current detection, poor thermal conductors are more desirable as scattering objects than materials with high thermal conductivity.

It can be seen that metals, particularly those used as electrical conductors, are not suitable as objects of study with infrared current detectivity. Materials such as copper, aluminum and silver are highly conductive both thermally and electrically, so the induced currents on a surface composed of one of these metals will produce very little heating. What little heat is produced will be very

rapidly and uniformly distributed over the surface of the metal due to the large value of thermal conductivity, k , for metals and the only detectable thermal change will be a very slight, uniform temperature rise on the metal's surface.

Even this uniform temperature change will be difficult to detect with an infrared detector due to the low emissivity for metals in the infrared region of the spectrum. Typical values of the emissivity constant, ϵ_{λ} , for these metals are .04 to .06 for polished aluminum, .02 for polished copper, and .02 for silver.

There are many studies in antenna design and placement, electromagnetic scattering, and electromagnetic compatibility where surface currents and charges must be determined. If the surface of metals could be treated or coated in such a way that made them suitable for infrared current detection techniques, this method of current determination could be directly applied to studies involving aircraft, ships, and other military equipment, or to metallic models of the equipment. Surface preparations of the appropriate thermal and electrical conductivity, emissivity, and reflectivity can be applied to nonmetallic models and yield accurate representations of the currents induced, as well.

B. THESIS OBJECTIVES

The goals of this work were to define the parameters of

suitable surface coatings so that infrared current detection methods could be applied to metal scattering objects, to determine what materials, if any, have these parameters, and to find suitable surface coatings for nonmetallic scatterers, apply them to more complex shapes and compare the results with results obtained by other methods.

II. EXPERIMENTAL APPARATUS

A. AGA THERMOVISION SYSTEM 680

The AGA Thermovision System 680 is an infrared camera and detection system manufactured by AGA Infrared Systems AB of Sweden. This system has been thoroughly discussed by Selim [2] and will be described in more general terms in this discussion. The system uses an Indium Antimonide photovoltaic detector, cooled by liquid nitrogen to 77°K. The detector is sensitive to infrared radiation in the range of two to 5.6 micron wavelengths.

The system scans the field of view using two octagonal prisms rotating on axes ninety degrees apart. The system processes the infrared radiation and produces real time, television-like displays on a color monitor and a black and white monitor. The system sensitivity is better than .2°C at 30°C. The black and white monitor displays the temperature profiles in white and shades of grey that progress towards black as the temperature decreases. The color monitor displays the temperature profiles in ten equal width color settings. The ordering of the colors from warmer to cooler can be adjusted by the operator to the arrangement that most clearly displays the information he is seeking. The system also includes a profile adaptor and display that displays the surface temperature cross section of any one of the horizontal scan lines, or all of the scan lines simul-

taneously on a diminished scale. The Thermovision system used in the laboratory was mounted on a tripod and the processing system was basically permanently mounted. However, AGA Infrared Systems also makes a Thermovision system that is entirely portable.

B. THERMOVISION DISPLAY INTERPRETATION

The Thermovision display has a temperature window with an adjustable width of from 1°C to 2000°C . This window can also be moved up or down the temperature scale as necessary, depending on the surface temperature of the object being viewed. The display divides this temperature window into ten different isotherms, the width of each isotherm being one tenth the width of the temperature window. On the color display, the color codes chosen by the operator are displayed across the bottom of the screen, starting from the coolest at the left and going toward the warmest on the right.

For permanent recording of information, a Polaroid camera can be attached to the front of the display. This camera produces color prints which have been converted to half tone black and white photographs for printing.

All photographs in this report use either $.1^{\circ}\text{C}$ isotherms or $.2^{\circ}\text{C}$ isotherms, and will be identified as they appear.

C. LABORATORY APPARATUS

The power source used to irradiate the scattering objects

was a Sierra Electronics Model 470A, with 80 watts maximum power output. The power source was connected via an isolator, dual directional coupler, and a dual stub tuner to a monopole antenna one quarter wavelength long at 937.5 MHz. This antenna was mounter near one end of a 3.8 by 11.5 wavelength (at 937.5 MHz) aluminum ground plane. A power meter was attached at the directional coupler's return port so that the reflected signal could be minimized by using the dual stub tuner. The operator was shielded from the antenna by a 60° corner reflector and by absorbing pads placed around the ground plane. The scattering objects were placed on the ground plane at a distance sufficiently far from the antenna so that the wave front was approximately plane. The half wavelength square flat plates were all placed 3.5 wavelengths from the antenna, while the cylinders were observed at different distances from the antenna. All objects placed on the ground plane were taped with copper tape to insure uniform electrical connections.

Since many of the resistive coatings commercially available did not have their conductivity specified, it was necessary to devise a method of measuring electrical conductivity. The resistance of a sheet of material of thickness d and length and width l is given by $R=l/\sigma d$ ohms. This resistance is measured between parallel sides as a square of this material, with electrical contact made all along the entire side. This value can then be substituted into the equation

and the value of the conductivity , σ , can be found. σ has units of mhos per meter. Electrical contacts of sufficient length were manufactured and a square of the material in question was attached to them. The resistance could be measured with an ohmmeter and the value of σ calculated.

One commonly used method of specifying a material's resistance is in "ohms per square". The "ohms per square" of a material will be given for a particular thickness and this will be the value of the resistance, independent of the size of the square. A one centimeter square will have the same resistance between parallel sides (electrical contact the entire length of the side) as does a one meter square of the material. This can be more easily seen if one considers incremental rows of incremental squares connected in series, with the rows connected in parallel. It can be seen that if the number of rows equals the number of incremental squares of resistance, the resistance is independent of the area of the total square.

III. SURFACE PREPARATIONS FOR METALS

A. USE OF OXIDE COATINGS AS A SURFACE PREPARATION FOR METAL SURFACES

Studies by Bramson [5] show that oxide coating on the surface of some metals greatly enhance the infrared emissivity of these surfaces. A graph prepared by Özisik, based on data from Gubareff, Janssen, and Torborg, [4] showing the effects of oxidation and temperature on the emissivity of metal surfaces is presented in Figure 1. Copper and brass are among those metals whose infrared properties are improved. The infrared emissivity of polished copper at room temperatures is .07, while for heavy layers of copper oxide, emissivity increases to .6 to .8 in the infrared region. For brass, with an emissivity of .06, the formation of a heavy oxide coating raises the emissivity to .61. Aluminum, on the other hand, has an especially low emissivity ($\epsilon_{\lambda} = .04$) and with heavy oxidation increases only to .2. Therefore, efforts to apply these findings to improving infrared current detection techniques concentrated on copper and brass.

Data provided by Bramson indicates that for brass, copper and other metals, sandblasting the surface or working the surface with emery increased the emissivity somewhat. Based on this information several sheets of copper were sandblasted to determine its effect on infrared current detection techniques.

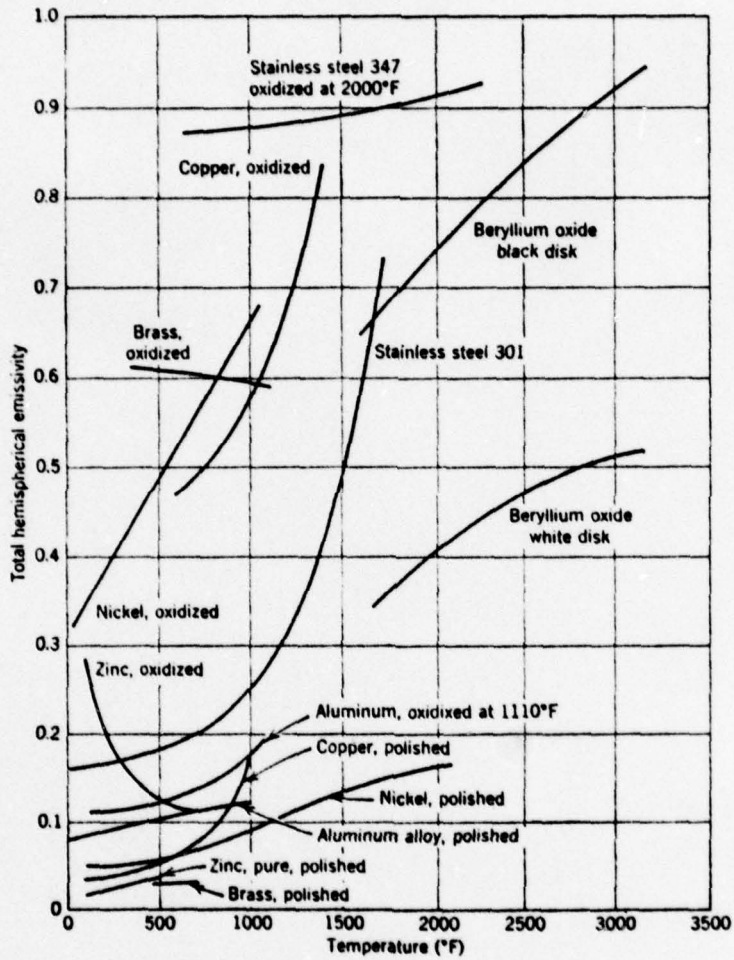


Figure 1. Graph compiled by Özisik from data given by Gubareff, Janssen, and Torborg [4] showing the effect of oxidation on emissivity.

1. Copper

a. Method of Formation of Oxide

It was decided to accelerate the oxidation process by heating the copper plate in an oven. It was found that an oven temperature of 300°C provided optimum conditions for oxidizing the copper. Higher temperatures yielded more fragile oxide coatings and the combination of high temperature and the difference in coefficients of thermal expansion for copper and copper oxide caused the oxide coating to separate from the copper as the sheet cooled. Temperatures below 300°C obviously yielded slower oxidation formation.

b. Results

The length of time the copper was subjected to the high temperature, and thus the amount of oxide formed, was varied as well as the preparation of the surface of the copper prior to oxidation. Half wavelength square copper plates were oxidized to different degrees and attached to the aluminum ground plane with copper tape. The plates were aligned such that the angle of incidence of the wavefront was 45°. The plates were then radiated by an antenna 3.5 wavelengths away at a frequency of 937.5 MHz, with an incident power level of 5 mw/cm². The plates were viewed with the AGA Thermovision 680 camera with these results.

(1) Pre-Polished Copper Plate Heated for Five Hours. The plate showed slight evidence of heating after

being irradiated for approximately five minutes. The heating was minimal and very uniform, and difficult to detect.

(2) Pre-Polished Copper Plate Heated for Nine Hours. The infrared emissivity increased with the increase in level of oxidation, but the amount of heating was again slight and uniform.

(3) Copper Plate With Natural Accumulation of Oxide Heated in Oven for Three Hours. The plate showed slight heating when irradiated. The heating was less uniform than with the other samples. The slight non-uniformity of the heating was due to the non-uniform oxidation on the plate prior to additional oxidation in the oven.

(4) Sand Blasted Copper Sheet, Unoxidized. The plate showed very slight and very uniform heating when irradiated.

(5) Sand Blasted Copper Sheet, Oxidized in an Oven. The sand blasted copper sheet was heated for three hours and the infrared camera showed moderate, uniform heating when the sheet was irradiated. After six hours of heating, the infrared camera showed an improvement in the amount of heating due to the incident electromagnetic radiation, but the heating remained very uniform. As predicted, oxidation and surface roughness increased the emissivity, but not the applicability to current detection.

2. Brass

a. Method of Formation of Oxide Coating

The oxidation process of the brass plate was accelerated in an oven in the same manner as the oxidation of the copper. For the same reasons that 300°C was an optimum temperature for copper plates, 490°C was found to be the optimum temperature for oxidizing the brass plates. Higher temperatures caused the plates to deform and the oxide coats were too fragile to be handled. The difference in the coefficients of thermal expansion of the brass plate and the oxide coat caused the coat to separate from the brass as it cooled. Lower temperatures yielded slower oxidation formation.

b. Results

As with the copper plate, the length of time the brass was subjected to the high temperature, and thus the amount of oxide formed, was varied. Half wavelength square brass plates were oxidized to different degrees and attached to the aluminum ground plane with copper tape. The plates were aligned such that the angle of incidence of the wavefront was 45°. The plates were then irradiated by an antenna 3.5 wavelengths away at a frequency of 937.5 MHz, with an incident power level of 5 cm/mw². The plates were viewed with the AGA Thermovision 680 camera with these results.

(1) Brass Plate Heated for Three Hours in Oven.

The plate showed no appreciable evidence of electromagnetically induced heating even after lengthy irradiation.

(2) Brass Plate Heated for Six Hours in Oven.

The plate showed no appreciable evidence of electromagnetically induced heating even after lengthy irradiation.

B. USE OF COPPER SULFIDE AS SURFACE PREPARATION

1. Method of Application

Half wavelength square copper plates were first mechanically cleaned with fine sandpaper to remove oxidation and surface contamination. After cleaning the plates were immersed in a moderately concentrated solution of zinc sulfide (ZnS). The entire plate was immersed in the solution at the same time in order that the copper sulfide coating would develop with uniform thickness on the plates' surface. After ten minutes the plates developed a thin, very black coating of copper sulfide. This procedure was conducted in a chemical fume hood.

2. Results

The half wave length square copper plate with the copper sulfide coating was attached to the conducting ground plane with copper tape 3.5 wavelengths from the radiating antenna, with the angle of incidence of the wavefront 45° from the normal of the plate. The incident power at the plate was 5 mw/cm^2 . After prolonged periods of irradiation, no appreciable heating was detected with the infrared camera.

C. RESISTIVE COATINGS AS PREPARATIONS FOR METAL SURFACES

Poor conductors (high resistance) are better suited to

infrared surface current detection procedures than good conductors since for a given current distribution more heat is generated, and the more heat generated the easier the current is to detect. Accordingly, coatings with much higher resistance than metals were tested as surface preparations for metal scatterers.

1. Television Tube Koat

Television Tube Koat is an aquadag coating manufactured by GC Electronics of Rockford, Illinois. It is lacquer based and available in aerosol spray and brush on form. It dries to a flat black finish and has good infrared emissivity. Its conductivity, as determined by procedures outlined in paragraph II.C., was found to be 160 mhos per meter.

a. Method of Application

The Television Tube Koat was sprayed onto the copper plate to form a uniform coat. The thickness of the coat was varied up to .026 mm and the resistive coat was placed both directly onto the copper plate and with an insulating layer between the copper and the Television Tube Koat.

b. Results

The half wavelength square plates with Television Tube Koat were placed on the conducting ground plane 3.5 wavelengths from the antenna and connected with copper tape. The plates were aligned so that the angle of incidence

of the wavefront was 45° . The incident power level at the plate was five mw/cm^2 . The plates were then irradiated for approximately five minutes each at a frequency of 937.5 MHz. For all thicknesses, with or without the insulating layer, moderate levels of uniform heating were observed. The heating was not sufficient to produce a good contrast with the background surfaces.

2. Carbon (Soot) Coating

Carbon has a conductivity of 10^4 mhos per meter, although in the less dense form of soot the conductivity will be lower. Carbon is an excellent emitter in the infrared region, with an emissivity of .93.

a. Method of Application

An oxygen-acetylene torch burning with the oxygen turned off produces large quantities of soot. The flame of the torch was moved across the surface of the metal plate and the soot deposit was built up in this manner. This method of application did not yield as uniform a layer of soot as desired, but sufficiently uniform so that contours arising from non-uniform coatings would not overshadow heating contours which might arise from induced current distributions.

b. Results

The soot-covered plates were attached to the conducting ground plane with copper tape at a distance of 3.5 wavelengths from the radiating antenna. The plates were

aligned so that the angle of incidence of the wavefront was 45° . The incident power was five mw/cm^2 . The plates were irradiated for approximately five minutes at a frequency of 937.5 MHz. For the brass plate coated with soot, there was little appreciable heating when irradiated. The copper plate showed some uniform heating when irradiated. A layer of Television Tube Coat, discussed previously in paragraph III.C.1.a., was applied on top of the soot coating on the copper plate. This combination yielded greater heating effects when radiated, but all heating was absolutely uniform.

3. Teledeltos Paper

Teledeltos paper is a resistive paper, $R_s = 2000$ ohms per square, with a thickness of 8.76×10^{-5} meters. This yields a conductivity of 5.7 mhos/meter. This gives a skin depth, δ , of 6.94×10^{-3} meters. Teledeltos paper has been shown to be effective in infrared current detection procedures when placed on a non-conducting surface [2].

a. Method of Application

Teledeltos paper can be applied easily and uniformly to flat plates, and can be applied in large thicknesses much more easily than the lacquer-type resistive coatings. In this case, 80 sheets of Teledeltos paper were attached to a half wavelength (16cm) square copper plate. This thickness was 13.8×10^{-3} meters, two skin depths thick. This plate was then placed on the conducting plane 3.5 wavelengths from the

antenna at an angle so that the incident wave arrived at the plate at an angle of 45° . Electrical connection with the ground plane was made with copper tape. The plate was then irradiated for several minutes at a frequency of 937.5 MHz with an incident power level of five mw/cm^2 .

b. Results

After several minutes of irradiation, the Teledeltos paper-covered plate showed isotherms in the areas where current densities were known to be at a maximum, but areas where current densities were known to be weaker were completely unchanged, and remained black, or cold, on the infrared camera display. This small amount of heating was slow to develop also. The resulting display did not represent the current densities that were known to exist for a flat plate scatterer.

D. ANALYSIS OF RESULTS OF METAL SURFACE PREPARATIONS

None of the surface preparations of the metal plates yielded satisfactory results. No evidence of heating contours (and hence surface current distributions) was produced with any of the surface preparations except the very thick layers of Teledeltos paper. Oxide coatings tended to increase the emissivity, with heavier oxide coatings yielding greater increases, as predicted by previously discussed experimental data. Surface preparations which increased the roughness of the surface, as did the sandblasting,

or decreased the reflectivity, as did the Television Tube Koat and soot also yielded increased emissivities as predicted. This increased emissivity was manifested in the greater evidence of heating detected on the plates. However, even the most dramatic of these increases in emissivity produced only slight heating in the plates, all of it very uniform and difficult to distinguish from the background.

The thick layer of Teledeltos paper ($d=2\delta$, approximately 14mm) covering was very slow to respond and produced heating contours which were limited to the areas where it was known that the maximum current densities were located. This indicates that there are two factors involved in the heating process, one involving electromagnetic properties of the material such as electrical conductivity and frequency of the incident wave, and another factor involving thermal properties of the material, such as thermal conductivity. The combination of these two properties imposes certain restrictions so that the use of preparations for metal surfaces for infrared current detection will be achievable only by the use of a surface coating within very specific thermal and electromagnetic parameters.

The electromagnetic problem will be approached by first examining the characteristics of a perfect conductor. It is known that for an electromagnetic wave incident on a perfect conductor, the wave is entirely reflected and none of the energy of the incident wave is transmitted to the perfect

The power source used to irradiate the scattering objects

conductor. Since there is no loss in a perfect conductor, no energy is absorbed. As the conductivity, σ , decreases from infinite, the electromagnetic wave begins to penetrate the conductor, but a good conductor sharply attenuates the wave and there is virtually no energy absorbed past the point where the attenuation is equal to e^{-4} , or four skin depths.

The skin depth, δ , of a good conductor is approximately

$$\delta = \sqrt{2/\omega\mu\sigma} \text{ meters}$$

The skin depth is defined as the depth at which the incident wave has been attenuated to $1/e$, or approximately 37% of the value transmitted across the boundary between the two media. For copper, the skin depth at 937.5 MHz is

$$\delta \approx \sqrt{\frac{2}{\omega\mu\sigma}} = 2.15 \text{ } \mu\text{m}$$

The transmission coefficient of the air to copper boundary is $.00000196/45^0$ for electric field. The ratio of the electric field to the magnetic field just inside the metal is η_{Cu} , the characteristic impedance of copper, and has a value of $.000369/45^0$ ohms. For most purposes this would be considered a zero impedance medium. Even taking the losses into account, only a very small amount of energy is transmitted from the incident wave and absorbed by the copper. Therefore the currents that are induced will be small and will produce very little heating. Additionally, the high thermal conductivity of the copper will cause this slight heating to be uniformly distributed at a very rapid rate, and the thermal effects of the induced currents will be very

difficult to detect.

The situation that arises when a resistive coating is applied is illustrated in Figure 2. The wave incident on boundary one between the air and the resistive coating is partially reflected and partially transmitted. The portion that is transmitted is

$$E_{T1}(z) = e^{-\alpha_T z} (|T_1| e^{j\theta_{T1}} E_i) e^{-j\beta z}$$

where $|T_1| e^{j\theta_{T1}}$ is the magnitude and phase of the transmission coefficient of the electric field at boundary one.

This can be expressed as

$$E_{T1}(z) = e^{-\alpha_T z} E_{T1} e^{-j\beta z}, \quad E_{T1} = |T_1| E_i e^{j\theta_{T1}}$$

where E_{T1} is a complex quantity.

Fields are attenuated in a lossy medium by a factor $e^{-\alpha z}$ where

$$\alpha = \text{Re} \{ \sqrt{j\omega\mu(\sigma + j\omega\epsilon)} \}$$

The transmitted waves propagate through the resistive coating and are attenuated as $e^{-\alpha_T z}$, where α_T is the attenuation constant for the resistive coating. When the wave reaches boundary two, $z=d$, where the resistive coating and the copper join, the wave is once again partially reflected and partially transmitted. The magnitude of the reflection coefficient at boundary two is very close to minus one, even for the maximum value of σ_R for any resistive coating used. However, in order to perform an exact analysis of field distributions, a resistive coating-copper boundary with a re-

reflection coefficient $|R_2|e^{j\theta_{R2}}$ for the electric field will be considered. The corresponding transmission coefficient is $|T_2|e^{j\theta_{T2}}$.

The reflected field at boundary two is

$$E_{R2}(z) = e^{-\alpha_T(d-z)} (E_{T1} e^{-\alpha_T d} |R_2| e^{j\theta_{R2}}) e^{j\beta z}$$

where $e^{-\alpha_T(d-z)}$ is the attenuation for a wave traveling in the $-z$ direction from $z=d$ to $z=0$.

The electric field transmitted into the copper is given

by

$$E_{T2}(z) = (E_{T1} e^{-\alpha_T d} |T_2| e^{j\theta_{T2}}) e^{-j\beta z} e^{-\alpha_{cu} z}$$

The total field in the resistive coating is given by

$E_{TOT} = E_{T1}(z) + E_{R2}(z)$ for $0 \leq z \leq d$, neglecting any further reflections.

$$E_{TOT} = e^{-\alpha_T z} (|T_1| E_i e^{j\theta_{T1}}) e^{-j\beta z} + e^{-\alpha_T(d-z)} (E_{T1} e^{-\alpha_T d} |R_2| e^{j\theta_{R2}}) e^{j\beta z}$$

Since both the resistive coating and the copper are conductive, the current density J , in amperes/ m^2 is given by $J = \sigma e$, where σ_R is the conductivity of the resistive coating and σ_{cu} is the conductivity of copper.

The current density in the resistive coating is given by

$$J_R(z) = e^{-\alpha_T z} (\sigma_R |T_1| E_i e^{j\theta_{T1}}) e^{-j\beta z} + e^{-\alpha_T(d-z)} (\sigma_R E_{T1} e^{-\alpha_T d} |R_2| e^{j\theta_{R2}}) e^{j\beta z}$$

and the current density in the copper is

$$J_{cu}(z) = (\sigma_{cu} E_{T1} |T_2| e^{-\alpha_T d} e^{j\theta_{T2}}) e^{-j\beta z} e^{-\alpha_{cu} z}$$

The amount of power absorbed, and hence the heating produced in the copper can be found by examining the current density J of the copper. In the copper $\frac{1}{\alpha} = \frac{1}{\beta} = \delta$, the skin depth.

$$J_{cu}(z) = (\sigma_{cu} E_{T1} |T_2| e^{-\alpha_T d} e^{j\theta_{T2}}) e^{-(1+j)z/\delta}$$

Total current per unit width in the y direction is

$$\int_0^{\infty} J_{cu}(z) dz \frac{\text{amperes}}{\text{meter}} = \sigma_{cu} E_T |T_2| e^{-\alpha_T d} e^{j\theta_{T2}} \int_0^{\infty} e^{-z/\delta(1+j)} dz$$

$$\text{Integrating, } \sigma_{cu} E_{T1} |T_2| e^{-\alpha_T d} e^{j\theta_{T2}} \left(\frac{-\delta}{j1+1} \right) e^{-(1+j)z/\delta} \Big|_0^{\infty}$$

$$= \sigma_{cu} E_{T1} |T_2| e^{-\alpha_T d} \frac{\delta}{\sqrt{2}} e^{j\pi/4} e^{j\theta_{T2}}$$

$$= e^{-\alpha_T d} \sigma_{cu} E_i |T_1| |T_2| e^{j(\theta_{T1} + \theta_{T2})} \frac{\delta}{\sqrt{2}} e^{-j\pi/4} =$$

$$e^{-\alpha_T d} \sigma_{cu} E_i |T_1| |T_2| \frac{\delta}{\sqrt{2}} e^{j(\theta_{T1} + \theta_{T2} - \pi/4)}$$

$$\frac{\text{total current}}{\text{unit width}} = d^{-\alpha_T d} \frac{\sigma_{cu} E_i |T_1| |T_2| \delta}{\sqrt{2}} \cos(\omega t + \theta_{T1} + \theta_{T2} - 45^\circ)$$

Now is this were distributed uniformly over a thickness, δ ,

$$\delta = e^{-\alpha_T d} \sigma_{cu} E_i |T_1| |T_2| \cos(\omega t + \theta) \text{ amp/m}^2$$

where $\theta = (\theta_{T1} + \theta_{T2} - 45^\circ)$. J is uniform over the thickness δ .

Instantaneous energy absorbed per unit volume = $J^2/\sigma \frac{\text{watts}}{\text{m}^3}$

$$\frac{J^2}{\sigma_{\text{cu}}} = e^{-\alpha_T 2d} \frac{\sigma_{\text{cu}} E_i^2 |T_1|^2 |T_2|^2}{2} \cos^2(wt + \theta)$$

The average value of $\cos^2(wt + \theta) = \frac{1}{2}$.

Average power absorption per unit volume is given by

$$\frac{P}{\text{vol}} = \frac{\sigma_{\text{cu}} E_i^2 |T_1|^2 |T_2|^2}{4} e^{-\alpha_T 2d} \frac{\text{watts}}{\text{m}^2}$$

The power absorption in a volume unit x unit $x \delta$ yields the power loss per square meter of surface area of the resistive coating - copper boundary.

$$\frac{P}{\text{m}^2} = \frac{\sigma_{\text{cu}} E_i^2 |T_1|^2 |T_2|^2 \delta}{4} e^{-\alpha_T 2d}$$

Values of these constants for typical resistive coating are as follows:

1. $|T_1|$ (at boundary of air and resistive coating) = .0356
2. $|T_2|$ (at boundary of resistive coating and copper) = .00331
3. $\sigma_{\text{cu}} = 5.8 \times 10^7$ mhos/m
4. $\alpha_T = 1.09 \times 10^3 \text{ m}^{-1}$
5. $\delta_T = 9.18 \times 10^{-4} \text{ m}$

These values give an absorption in the copper of

$$\frac{P}{\text{m}^2} = 4.35 \times 10^{-7} e^{-\alpha_T 2d} E_i^2 \text{ watts/m}^2$$

for $d = 2\delta_T$

$$\frac{P}{m^2} = 7.97 \times 10^{-9} E_i^2 \text{ watts/m}^2$$

$$\text{for } d = .05\delta_T$$

$$\frac{P}{m^2} = 3.93 \times 10^{-7} E_i^2 \text{ watts/m}^2$$

So the power absorbed in the copper varies from $3.93 \times 10^{-7} E_i^2$ watts per square meter of surface area of the resistive coating for a thin resistive coat ($d=.05\delta$) to 7.97×10^{-9} watts per square meter of surface area for a sheet of resistive coating two skin depths thick.

Consider now the power absorbed (and the heating produced) in the resistive spray.

$$J_R(z) = e^{-\alpha_T z} (\sigma_R |T_1| E_i e^{j\theta_{T1}}) e^{-j\beta z} + e^{-\alpha_T(d-z)} (\sigma E_T e^{-\alpha_T d} |R_2| e^{j\theta_{R2}}) e^{j\beta z}$$

$$J_R(z) = e^{-\alpha_T z} (\sigma_R |T_1| E_i e^{j\theta_{T1}}) e^{-j\beta z} + e^{-\alpha_T(d-z)} (\sigma_R |T_1| e^{j\theta_{T1}} E_i e^{-\alpha_T d} |R_2| e^{j\theta_{R2}}) e^{j\beta z}$$

$$J_R(z) = \sigma_R |T_1| E_i e^{j\theta_{T1}} (e^{-\alpha_T z} e^{-j\beta z} + e^{-\alpha_T(d-z)} e^{-\alpha_T d} |R_2| e^{j\theta_{R2}} e^{j\beta z})$$

$$J_R(z) = \sigma_R |T_1| E_i e^{j\theta_{T1}} (e^{-z(\alpha_T + j\beta)} + e^{-2\alpha_T d} |R_2| e^{j\theta_{R2}} e^{z(\alpha_T + j\beta)})$$

$$\frac{\text{Total I}}{\text{unit width}} = \sigma_R |T_1| E_i e^{j\omega T_1} \left[\int_0^d e^{-z(\alpha_T + j\beta)} dz + \right.$$

$$\left. \int_0^d e^{-2\alpha_T d} e^{z(\alpha_T + j\beta)} |R_2| e^{j\omega R_2} dz \right] \frac{\text{amps}}{\text{m}}$$

$$= \sigma_R |T_1| E_i e^{j\omega T_1} \left[\frac{e^{-z(\alpha_T + j\beta)}}{-(\alpha_T + j\beta)} \right]_0^d + |R_2| e^{j\omega R_2} e^{-2\alpha_T d}$$

$$\frac{e^{z(\alpha_T + j\beta)}}{\alpha_T + j\beta} \left[\right]_0^d \frac{\text{amps}}{\text{m}}$$

$$= \frac{\sigma_R |T_1| E_i e^{j\omega T_1}}{\alpha_T + j\beta} \left[e^{-d(\alpha_T + j\beta)} + 1 + |R_2| e^{j\omega R_2} e^{-2\alpha_T d} \right. \\ \left. (e^{d(\alpha_T + j\beta)} - 1) \right] \frac{\text{amps}}{\text{m}}$$

This can be expressed as

$$\frac{\text{I Total}}{\text{unit width}} = \frac{\sigma_R |T_1| E_i}{\sqrt{2} \alpha_T} \left[\cos(\omega t - 45^\circ) - |R_2| e^{-2\alpha_T d} \cos(\omega t + \phi_3) \right. \\ \left. - e^{-\alpha_T d} \cos(\omega t + \phi_2) + |R_2| e^{-2\alpha_T d} \cos(\omega t + \phi_1) \right] \frac{\text{amps}}{\text{m}}$$

where $\phi_1 = \theta_{T1} + \theta_{R2} - 45^\circ - \beta d$, $\phi_2 = \theta_{T1} - 45^\circ - \beta d$ and

$$\phi_3 = \theta_{T1} + \theta_{R2} - 45^\circ$$

Distributed uniformly over a depth, δ ,

$$J = \frac{I}{m^2} = \frac{\sigma_R |T_1| E_i}{\sqrt{2} \alpha_T \delta} \left[\cos(\omega t - 45^\circ) - |R_2| e^{-2\alpha_T d} \cos(\omega t + \phi_3) - e^{-\alpha_T d} \cos(\omega t + \phi_2) + |R_2| e^{-2\alpha_T d} \cos(\omega t + \phi_1) \right] \frac{\text{amps}}{m^2}$$

$\frac{J^2}{\sigma}$ yields instantaneous power loss.

Taking the time average of $\frac{J^2}{\sigma}$ yields the following expression for total average power absorbed per unit volume in the resistive coating.

$$J^2 \cdot \frac{1}{\sigma_R} = \frac{\sigma_R |T_1|^2 E_i^2}{2\alpha_T^2 \delta^2} \left[\frac{1}{2} + \frac{|R_2|^2 e^{-4\alpha_T d}}{2} + \frac{e^{-2\alpha_T d}}{2} + \right.$$

$$\left. \frac{|R_2|^2 e^{-4\alpha_T d}}{2} \right]$$

$$\left. - |R_2| e^{-2\alpha_T d} \cos(\phi_3 + 45^\circ) - e^{\alpha_T d} \cos(\phi_2 + 45^\circ) + |R_2| e^{-2\alpha_T d} \cos(\phi_1 + 45^\circ) \right] \frac{w}{m^3}$$

The following values of material parameters are typical for the resistive coatings used.

1. $R_2 \angle_{R2}^{\circ} = .9969 \angle_{180.001}^{\circ}$
2. $T_1 \angle_{T1}^{\circ} = .0356 \angle_{44.27}^{\circ}$
3. $\sigma_R = 160 \text{ mho/meter}$
4. $\delta = \frac{1}{\alpha_T} = \frac{1}{\beta_T} = 9.18 \times 10^{-4} \text{ m}$

The power absorbed per square meter of resistive coating is given by

$$\left[\frac{I}{\text{m}^2} \right]^2 \frac{d}{\sigma_R} \frac{\text{watts}}{\text{m}^2}$$

Examining this power absorption for $d = .05\delta$, approximately .05 mm, we find the total power absorbed by the resistive coating to be $9.819 \times 10^{-7} E_i^2$ watts per square meter of surface area of the coating. For a thickness $d = 2\delta$, the power absorbed by the resistive coating is $8.842 \times 10^{-5} E_i^2$ watts per square meter of surface area, almost one hundred time greater than the power absorption of the thinner coating.

It is seen that the power absorption in the resistive coating varies with the thickness. For a thin layer there is very little attenuation, and due to the minus one reflection coefficient at the resistive coating - copper boundary, the values of the incident and reflected wave within the coating very nearly cancel. As the thickness of the resistive coating approaches twice the skin depth of the

resistive coating, there is a much greater attenuation for both the incident and reflected wave. Because of this attenuation the magnitudes of the incident and reflected waves are not the same, there is much less cancellation, and the resultant fields in the resistive coating are much stronger. This results in more power loss in the coating and more heating produced.

Recall that when a 2δ thickness of Teledeltos paper was applied to the copper plate, temperature profiles were produced, but only in the area where current densities were known to be of large magnitude. Most of the surface of the plate did not produce temperature changes of sufficient magnitude to be detected. The requirements resulting from electromagnetic aspects of this problem were satisfied but the thermal aspects of the problem prevented a sufficient rise in surface temperatures.

In order to investigate the temperature distribution and thus find the surface temperatures that result on the flat plate scatterer the power per unit volume as a function of z must be known. The formula for the current density as a function of z and t in the resistive coating was found to be

$$J_R(z, t) = \sigma_R |T_1| E_i \cos(\omega t - \beta_R z + \theta_{T1}) e^{-\alpha_R z} + e^{-\alpha_R (d-z)} (\sigma_R E_i |T_1| |R_2| e^{-\alpha_R d} \cos(\omega t + \beta_R z + \theta_{R2} + \theta_{T1}))$$

substituting $\frac{1}{\delta} = \beta_R = \alpha_R$, squaring $J_R(z,t)$, and dividing by σ_R , the following expression for power per unit volume results.

$$\begin{aligned} \frac{J^2(z,t)}{\sigma_R} = & \sigma |T_1|^2 E_i^2 \cos^2(\omega t + \theta_{T1} - z/\delta) e^{-2z/\delta} + \\ & 2 |R_2|^2 e^{-2d/\delta} \cos(\omega t - z/\delta + \theta_{T1}) \cos(\omega t + z/\delta + \theta_{R2} + \theta_{T1}) + \\ & |R_2|^2 e^{-2d/\delta} \cos^2(\omega t + z/\delta + \theta_{R2} + \theta_{T1}) e^{-2(d-z)/\delta} \end{aligned}$$

For $t=0$,

$$\begin{aligned} \frac{J^2(z,0)}{\sigma_R} = & \sigma_R |T_1|^2 E_i^2 \cos^2(\theta_{T1} - z/\delta) e^{-2z/\delta} + \\ & 2 |R_2|^2 e^{-2d/\delta} \cos(\theta_{T1} - z/\delta) \cos(\theta_{R2} + \theta_{T2} + z/\delta) + \\ & |R_2|^2 e^{-2d/\delta} \cos^2(z/\delta + \theta_{R2} + \theta_{T1}) e^{-2(d-z)/\delta} \end{aligned}$$

Graphs of these curves are plotted in Figure 3.

For $d=2\delta$, the second and third terms are multiplied by a factor of e^{-4} and can be ignored. This leaves

$$\frac{J^2(z,0)}{\sigma_R} \approx \sigma_R |T_1|^2 E_i^2 (\cos^2(\theta_{T1} - z/\delta) e^{-2z/\delta}) \frac{\text{watts}}{m^3}$$

which can be expressed as

$$\frac{J^2(z,0)}{\sigma_R} \approx \sigma_R |T_1|^2 E_i^2 (\frac{1}{2} + \frac{1}{2} \cos 2(\theta_{T1} - z/\delta)) e^{-2z/\delta} \frac{\text{watts}}{m^3}$$

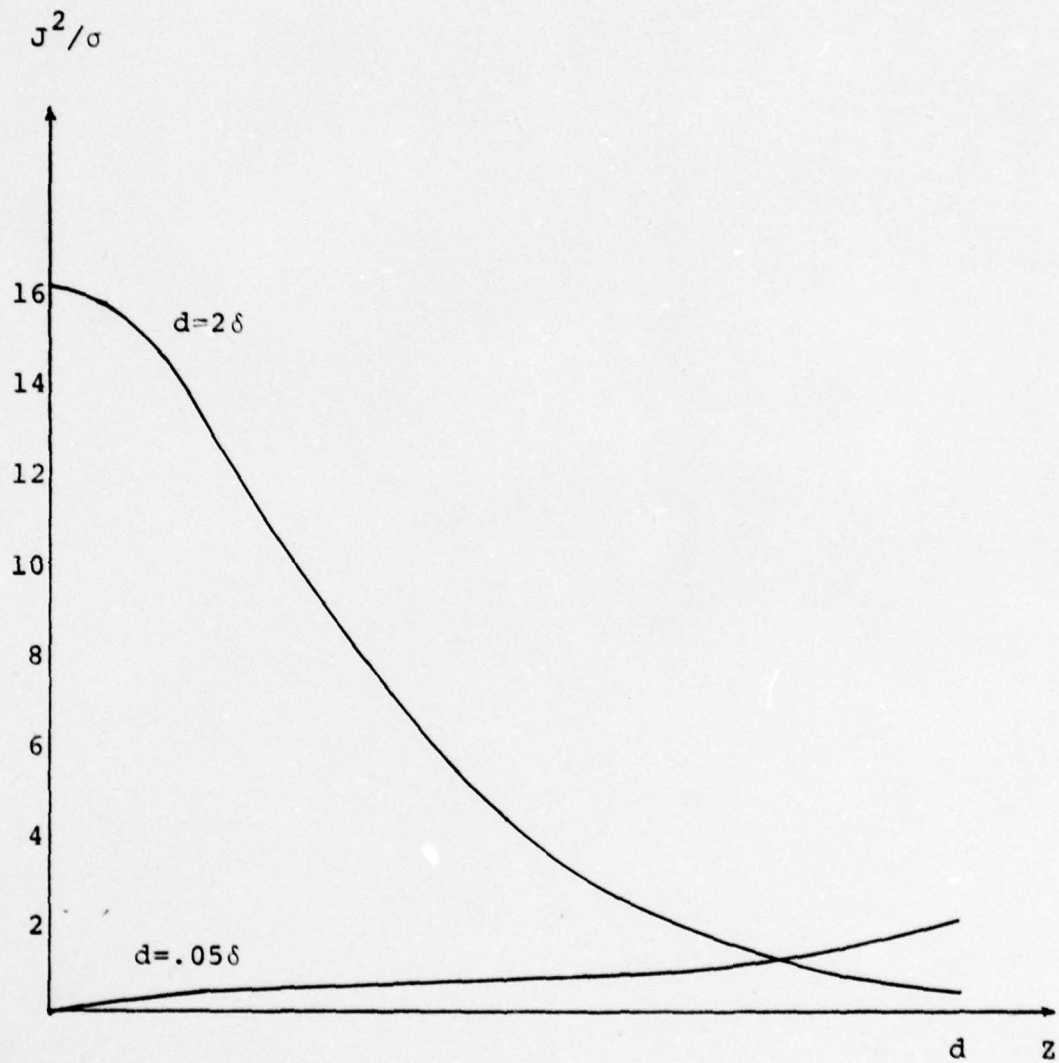


Figure 3. J^2/σ for $d=.05\delta$ and $d=2\delta$). The magnitude on the vertical scale is a relative magnitude for comparison for the two curves.

Ignoring the damped cosine curve introduces a small error but the distribution still has basically the same shape as a decaying exponential and the value of the function at $z=0$ is not changed by ignoring the cosine term. Therefore,

$$\frac{J^2(z,0)}{\sigma_R} \approx \frac{\sigma_R |T_1|^2 E_1^2 e^{-2z/\delta}}{2}$$

In order to derive an expression for the temperature distribution it will be assumed that the thickness of the resistive coating is much less than the other dimensions of the coating. To analyze the temperature distribution in the z direction, the geometric current density variations on the surface of the plate in the x and y directions and the resulting variations in power per unit volume in the x and y directions will be ignored. The goal of the analysis is to examine the manner in which the thermal properties of the material affect the surface temperature for a given power density ($\Delta J^2/\sigma_R$). This influence on the surface temperature will be of the same form regardless of power density, and therefore nothing is to be gained at this point by considering current density variations in the x and y directions.

The general equation for the temperature in the resistive spray is $k\nabla^2 T + Q'''(x,y,z) = 0$ where k is the thermal conductivity with units of watts/m²°C, T is temperature in °C and $Q'''(z,y,z)$ is the heat generated in the material in units of watts/m³. For the one dimensional

problem under consideration, the geometry of which is shown in Figure 2,

$$k \frac{d^2 T}{dz^2} + Q'''(z) = 0$$

$$Q'''(z) = \frac{J^2(z,0)}{\sigma_R} = \frac{\sigma |T_1|^2 E_i^2}{2} e^{-2z/\delta} \quad \frac{\text{watts}}{\text{m}^3}$$

$$\text{Let } A = \frac{\sigma |T_1|^2 E_i^2}{2} \quad \frac{\text{watts}}{\text{m}^3}$$

$$(1) \quad k \frac{d^2 T}{dz^2} + A e^{-2z/\delta} = 0$$

The boundary conditions are

$$(2) \quad h(T_a - T) = -k \frac{dT}{dz}, \quad z=0$$

$$(3) \quad T(z) = T_a \quad \text{at} \quad z=d.$$

where h is the heat transfer coefficient in units of $\frac{\text{watts}}{\text{m}^2 \cdot ^\circ\text{C}}$

and T_a is the ambient temperature of the air.

The boundary condition at $z=0$ equates the heat flow due to conduction at the boundary ($-k \frac{dT}{dz}$, $z=0$) to the convective heat flow from the plate to the air at the boundary. At $z=d$, the boundary between the copper and the resistive coating, the temperature can be assumed to be the ambient temperature, due to the extremely high thermal conductivity of the copper.

Integrating Eq (1),

$$(4) \quad \frac{dT}{dz} = \frac{A}{k} \left(\frac{-\delta}{2}\right) e^{-2z/\delta} + C_1$$

Integrating Eq (4),

$$(5) \quad T = \frac{-A}{k} \left(\frac{\delta^2}{4}\right) e^{-2z/\delta} + C_1 z + C_2$$

Substitute Eqs (4) and (5) into Eq (2), yielding

$$h \left(T_a + \frac{A\delta^2}{4k} e^{-2z/\delta} + C_1 z + C_2 \right) = -k \left(\frac{A\delta}{2k} e^{-2z/\delta} + C_1 \right), \quad z=0$$

Substituting Eq (5) into Eq (3),

$$T_a = \frac{-A\delta^2}{4k} e^{-2z/\delta} + C_1 z + C_2, \quad z=d$$

For the appropriate values of z ,

$$(6) \quad h \left(T_a + \frac{A\delta^2}{4k} - C_2 \right) = -k \left(\frac{A\delta}{2k} + C_1 \right)$$

and

$$(7) \quad T_a = \frac{-A\delta^2}{4k} e^{-2d/\delta} + C_1 d + C_2$$

Rearranging (6),

$$C_1 = \frac{-h}{k} \left(T_a + \frac{A\delta^2}{4k} - C_2 \right) \frac{-A\delta}{2k}$$

Substituting into Eq (7),

$$C_2 = T_a + \frac{A\delta^2}{4k} e^{-2d/\delta} + \frac{hd}{k} \left(T_a + \frac{A\delta^2}{4k} - C_2 \right) + \frac{A\delta d}{2k}$$

$$(8) \quad C_2 = T_a + \frac{A\delta^2}{4k} \left(\frac{hd}{k} + e^{-2d/\delta} \right) \left(\frac{1}{1 + \frac{hd}{k}} \right) + \frac{A\delta d}{2k} \left(\frac{1}{1 + \frac{hd}{k}} \right)$$

$$(9) \quad C_1 = \frac{-h}{k} \left(T_a + \frac{A\delta^2}{4k} - C_2 \right) - \frac{A\delta}{2k}$$

Substituting Eq (8) into Eq (9) and simplifying,

$$C_1 = \frac{-h}{k} \frac{A\delta^2}{4k} \left(\frac{1-e^{-2d/\delta}}{1+\frac{hd}{k}} \right) + \frac{A\delta}{2h(1+\frac{hd}{k})}$$

Substituting Eqs (8) and (10) into Eq (5),

$$T(z) = A \left[\frac{-\delta^2}{4k} e^{-2z/\delta} - \frac{h}{(1+\frac{hd}{k})} \left(\frac{\delta^2(1-e^{-2d/\delta})}{4k} \right) + \frac{\delta}{2h} z + \frac{T_a}{A} + \frac{\delta^2}{4k} \left(\frac{\frac{hd}{k} + e^{-2d/\delta}}{1+\frac{hd}{k}} \right) + \frac{\delta d}{2k} \left(\frac{1}{1+\frac{hd}{k}} \right) \right]$$

This is plotted for various values of d in Figure 4. For $z=0$,

$$T(z) = T(0) = T_s = A \frac{-\delta^2}{4k} + \frac{T_a}{A} + \frac{\delta^2 \left(\frac{hd}{k} + e^{-2d/\delta} \right)}{4 \left(1 + \frac{hd}{k} \right)} + \frac{\delta d}{2k} \left(\frac{1}{1 + \frac{hd}{k}} \right)$$

It is found that for a given resistive coating the surface temperature T_s increases as d increases. As d gets very large, the surface temperature approaches a constant value. The surface of the resistive coating is relatively close to the copper plate for small values of d . Since the temperature of the copper is effectively held constant at T_a , when d is small the surface of the resistive coating is more strongly affected by the temperature of the copper. As d increases, the effect of the copper on the surface tempera-

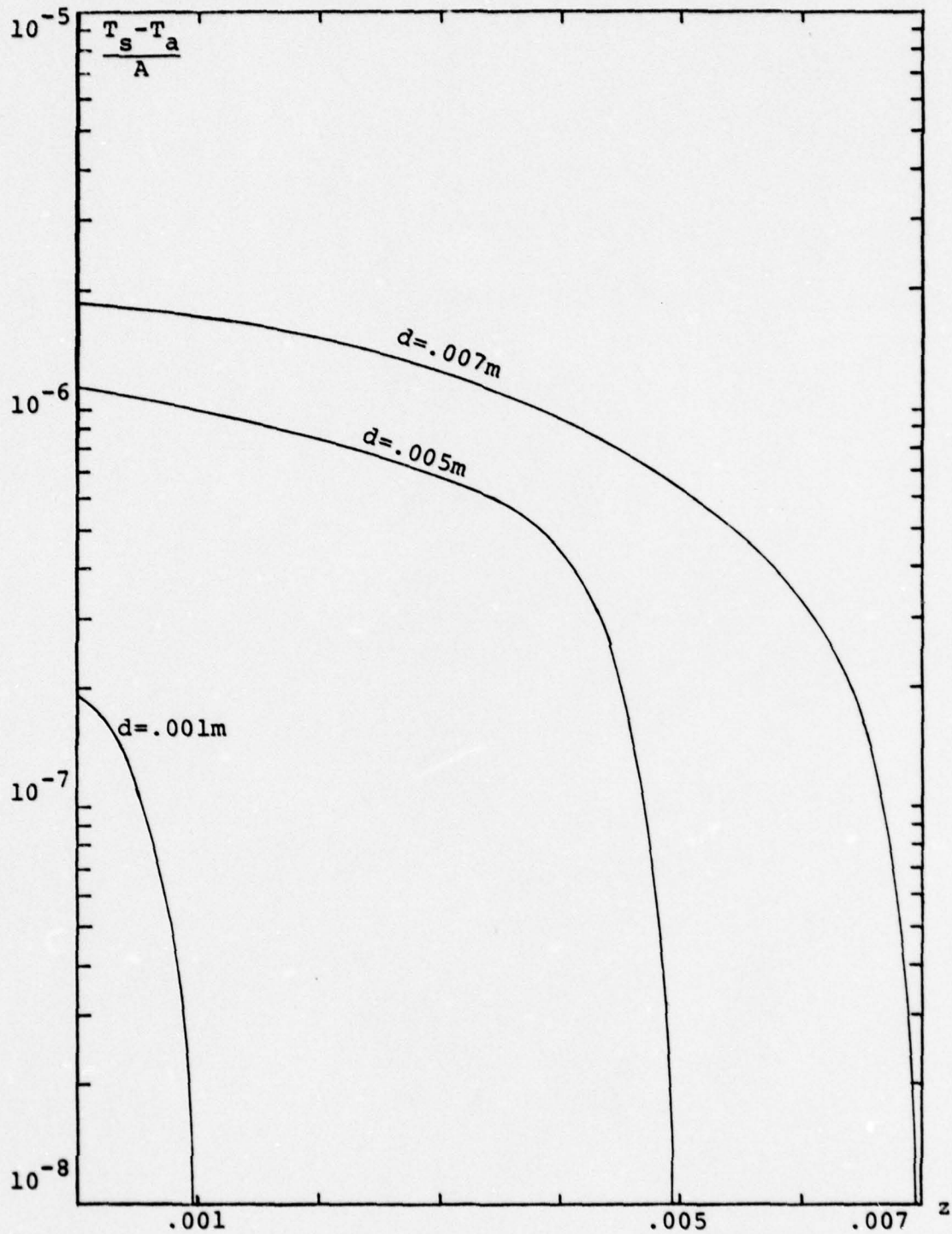


Figure 4. Temperature as a function of z for various thicknesses, d . Note the increase in surface temperature as d increases.

ture decreases until for sufficiently large d , the surface temperature is effectively independent of the temperature of the copper. The influence of the copper temperature on T_s is a function of the thermal conductivity, k . For k relatively large, conduction heat transfer in the coating is large and the effect of the copper temperature is greater. When k is relatively small, conduction heat transfer in the coating is small and the effect of the copper temperature is lessened.

This effect can be more clearly understood by studying an analogous electrical circuit, shown in Figure 5. The voltage at point two is fixed at ground potential. For a given current, the only way to increase the voltage at point one is to increase R . In the thermal problem with the copper plate, the temperature at $z=d$, at the copper plate, is analogous to the voltage at point two. The induced current density causing the heating is analogous to the current I . The surface temperature, T_s , can only be increased by increasing $\frac{d}{k}$, analogous to R , for a given current density.

In the case of the two skin depths of Teledeltos paper covering the copper plate, the thermal conductivity of the Teledeltos paper was sufficiently high so that the thickness of the Teledeltos paper was insufficient to isolate the surface temperature of the paper from the temperature of the copper plate. Since the thermal conductivity of the paper

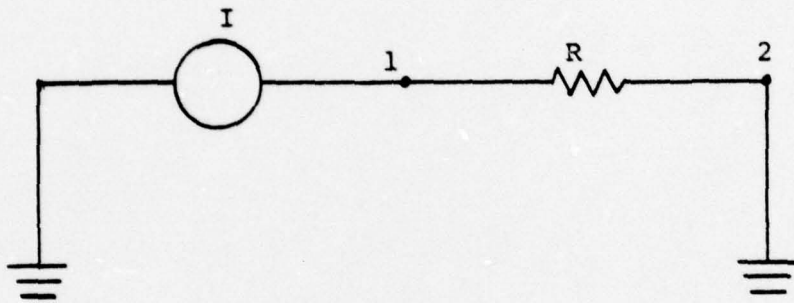


Figure 5. Electrical Analogue of the thermal restriction placed by copper sheet on the surface of the resistive coating.

is fixed, the only way to increase the surface temperature of the Teledeltos plate is to increase the thickness d .

Thus it has been determined that for a given frequency, electrical parameters of the material dictate that any surface preparation designed to enhance the applicability of infrared current detection on metal surfaces must have a certain minimum thickness, $d \geq 2\delta$. This δ then specifies an electrical conductivity σ . It has been further shown that thermal properties of the material require a specific relationship between the thickness, d , and the thermal conductivity, k , in order for temperature differences to arise on the surface that are sufficient for infrared detection. Therefore frequency and thickness specify the physical parameters of a surface coating required for satisfactory performance as a preparation for metal surface.

None of the substances tried in the experiments described in paragraphs III.A, B and C produced satisfactory results. This fact leads to the question, what is the exact relationship required between frequency, thickness and thermal and electrical conductivities for satisfactory performance? Further, after this relationship has been determined what materials, if any, satisfy this relationship?

To be a satisfactory coating, at least a $.2^{\circ}\text{C}$ change in the surface temperature must arise for the minimum difference in current densities that are desired to be detected. ΔJ (ΔJ will be defined as that minimum current

density difference desired to be detected) clearly depends on the anticipated spatial variation in current density and on the incident power.

A term A was defined previously to be equal to $\frac{\sigma |T_1|^2 E_i^2}{2}$ watts/m³. This is equivalent to $\frac{(J_{RMS})^2}{\sigma}$, also in units of watts per unit volume. If $A = \frac{(J_{RMS})^2}{\sigma}$, then $\Delta A = (\Delta J_{RMS})^2 / \sigma$ where ΔA is the power per unit volume at $z=0$ produced by the current density ΔJ_{RMS} (NOTE: Δ does not refer to differential quantities but to detectable levels of current and power densities).

In order to determine the variation of ΔA with frequency and electrical conductivity, ΔJ_{RMS} must be defined. For purposes of analysis, the minimum current density difference required to be detectable is $J_0/2$, where J_0 is the RMS current density produced by an incident electromagnetic wave with power incident = P_{inc} watts/m² on an infinite flat plate of the surface preparation.

$$J_0 = \frac{\sigma_R |T_1| E_i}{\sqrt{2}} \frac{\text{amps}}{\text{m}^2} \quad \text{where}$$

$$E_i = \sqrt{2 \eta_{air} P_{inc}} \frac{\text{v}}{\text{m}} \quad \text{and}$$

$$|T_i| = \frac{2 \eta_{coating}}{\eta_{air}} = \frac{2}{\eta_{air}} \left| \sqrt{\frac{j \omega \mu}{\sigma + j \omega \epsilon}} \right|$$

$$T_i = \frac{2}{\eta_{air}} \left| \frac{\sqrt{2 \pi f \mu}}{\sqrt{\sigma + j 2 \pi f \epsilon}} \right|$$

$$\Delta J_{\text{RMS}} = \frac{J_0}{2} = \left(\frac{\sigma}{2\sqrt{2}} \sqrt{2\eta_{\text{air}} P_{\text{inc}}} \right) \frac{2}{\eta_{\text{air}}} \frac{\sqrt{2\pi f \mu}}{|\sqrt{\sigma + j2\pi f \epsilon}|}$$

$$\frac{\Delta J_{\text{RMS}}}{\sigma} = \frac{2}{\eta_{\text{air}}} \frac{P_{\text{inc}} 2\pi f \mu}{|\sigma + j2\pi f \epsilon|}$$

It can be seen that for a given ΔJ the resulting ΔA increases as σ increases until σ becomes greater than 10 mhos/m, at which point ΔA is effectively independent of σ . The resulting ΔA also increases as the frequency increases. ΔA is more sensitive to frequency changes when σ is fairly large (greater than 2 mhos/m). The relationship between the ΔA produced for a given ΔJ , frequency, and conductivity are shown in Figure 6, where $\Delta J = J_0/2$, J_0 being produced by $P_{\text{inc}} = 10\text{mw}/\text{cm}^2$.

This same term A is found in the equation for the surface temperature of the coating.

$$T_s = T_a + A \left[\frac{\delta^2}{4k} \frac{\left(\frac{hd}{k} + e^{-2d/\delta} \right)}{\left(1 + \frac{hd}{k} \right)} + \frac{\delta d}{2k} \left(\frac{1}{1 + \frac{hd}{k}} \right) - \frac{\delta^2}{4k} \right]$$

The increase in surface temperature above the ambient temperature is $T_s - T_a$.

$$T_s - T_a = A \left[\frac{\delta^2}{4k} \frac{\left(\frac{hd}{k} + e^{-2d/\delta} \right)}{\left(1 + \frac{hd}{k} \right)} + \frac{\delta d}{2k} \left(\frac{1}{1 + \frac{hd}{k}} \right) - \frac{\delta^2}{4k} \right]$$

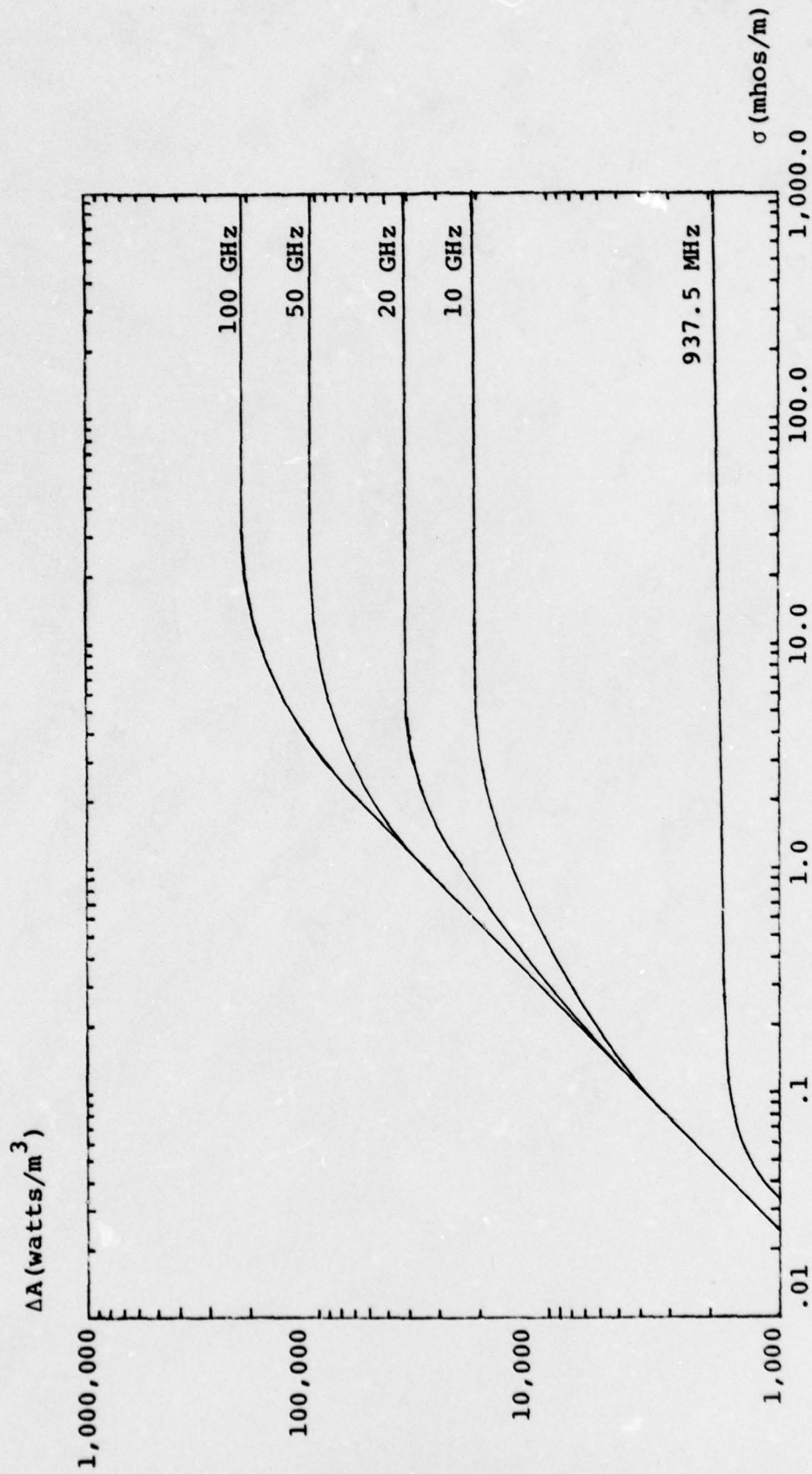


Figure 6. Graph showing ΔA produced for a given ΔJ with resistive coating with conductivity at frequency f .

If a $.2^{\circ}$ temperature rise above ambient is required for given values of δ , h , d , and k , then

$$A = .2 \left[\frac{\delta^2}{4k} \frac{\left(\frac{hd}{k} + e^{-2d/\delta}\right)}{\left(1 + \frac{hd}{k}\right)} + \frac{\delta d}{2k} \left(\frac{1}{1 + \frac{hd}{k}}\right) - \frac{\delta^2}{4k} \right]^{-1}$$

Define $\Delta A(.2)$ as the value of A which will produce a $.2^{\circ}$ temperature rise above ambient temperature for given parameters δ , k , h , and d .

$$\Delta A(.2) = .2 \left[\frac{\delta^2}{4k} \frac{\left(\frac{hd}{k} + e^{-2d/\delta}\right)}{\left(1 + \frac{hd}{k}\right)} + \frac{\delta d}{2k} \left(\frac{1}{1 + \frac{hd}{k}}\right) - \frac{\delta^2}{4k} \right]^{-1}$$

It can be seen that the same value of $\Delta A(.2)$ will produce a $.2^{\circ}$ temperature rise above ambient temperature regardless of the magnitude of the ambient temperature and that for a $.4^{\circ}$ temperature rise above ambient, $\Delta A(.4) = 2 \times \Delta A(.2)$.

As δ increases, the value of A required for a $.2^{\circ}\text{C}$ temperature rise decreases. However, δ is limited by the electromagnetic reflection problem to $\delta \leq d/2$. It is obvious that to minimize ΔA required for a $.2^{\circ}$ temperature change, $d \geq 2\delta$ is the optimum relationship between d and δ .

It can also be shown that for a constant δ and d at optimum conditions ($d=2\delta$), as k increases the required ΔA for a $.2^{\circ}\text{C}$ temperature change also increases and for a constant k as the thickness d is increased (keeping $\delta=d/2$) the required ΔA decreases. A lower k and/or greater thick-

ness d helps isolate the surface temperature T_s from the effects of the temperature of the copper. This relationship between k , d , and the required ΔA for a $.2^\circ\text{C}$ temperature change is shown by the graph in Figure 8.

At this point a ΔA produced by a given ΔJ is known and a $\Delta A(.2)$ required to produce a $.2^\circ\text{C}$ temperature change is known. Both ΔA and $\Delta A(.2)$ are defined in terms of the parameters of the coating and the frequency of the incident electromagnetic wave. In order for a $.2^\circ$ temperature rise to result from a ΔJ , and ΔA produced by the ΔJ must be greater than the $\Delta A(.2)$ required for a $.2^\circ\text{C}$ temperature rise.

In order to be able to determine what parameters of the coating are required for producing thermally detectable differences in current density, the information shown in Figures 6 and 7 are combined on the graph in Figure 8. Figure 8 shows the relationship between k , $\frac{1}{\sigma}$, and frequency for various values of ΔJ resulting from different incident power levels. For a given frequency curve, all points of the graph to the right of the curve represent acceptable combinations of thermal and electrical conductivity. It is seen that the required values of thermal and electrical conductivity are not very sensitive to changes in frequency. They are somewhat more sensitive to changes in the incident power level, which change ΔJ due to the definition of ΔJ in this analysis.

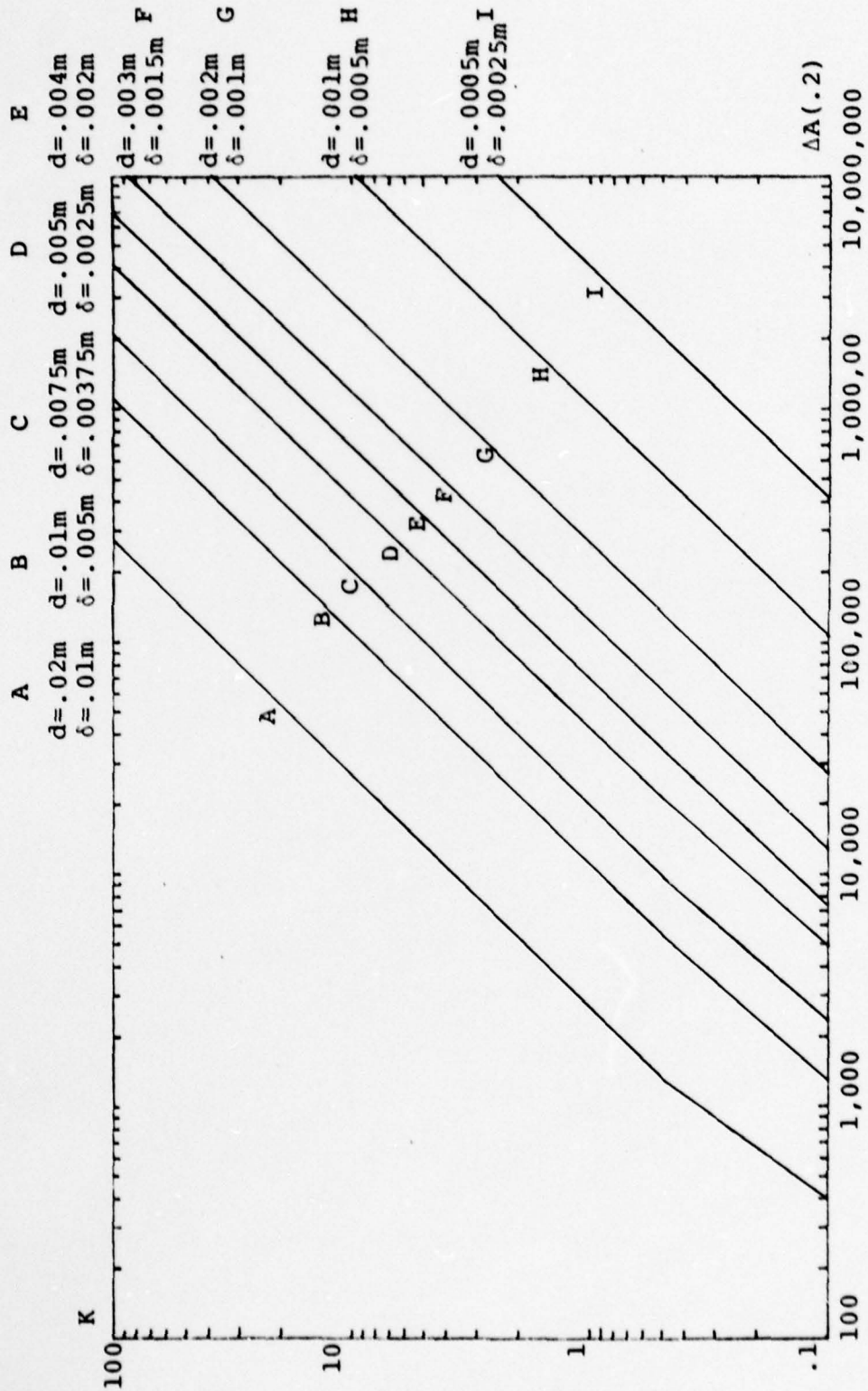


Figure 7. Graph showing the value of $\Delta A(.2)$ required for given values of k and d .

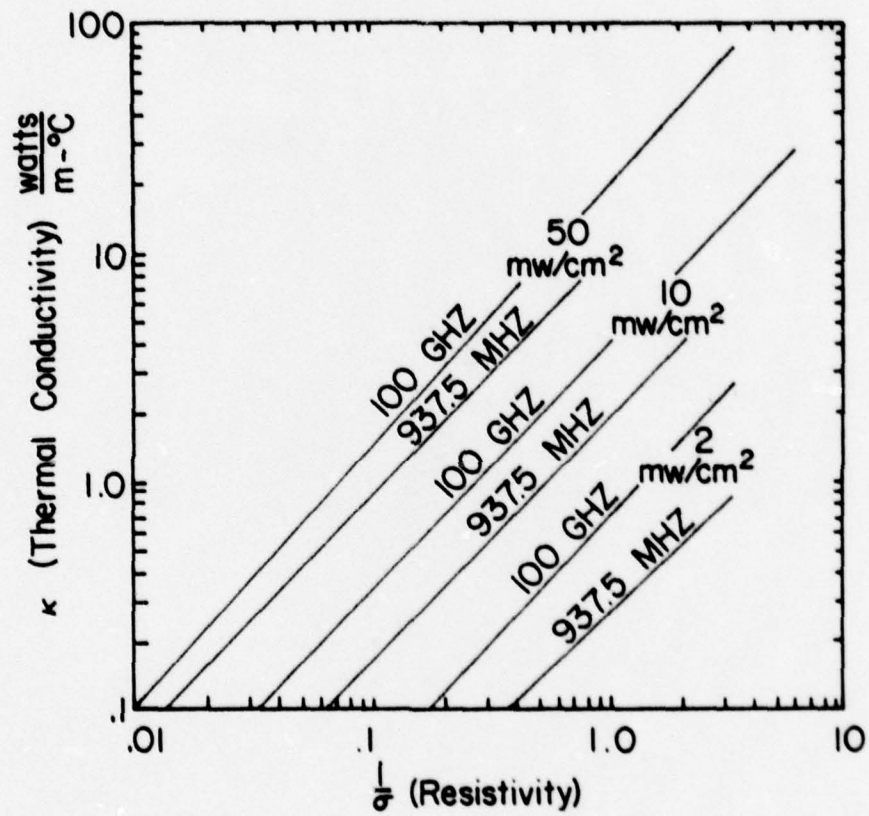


Figure 8. Regions of acceptable parameters of surface preparations for current detection on a perfect conducting surface

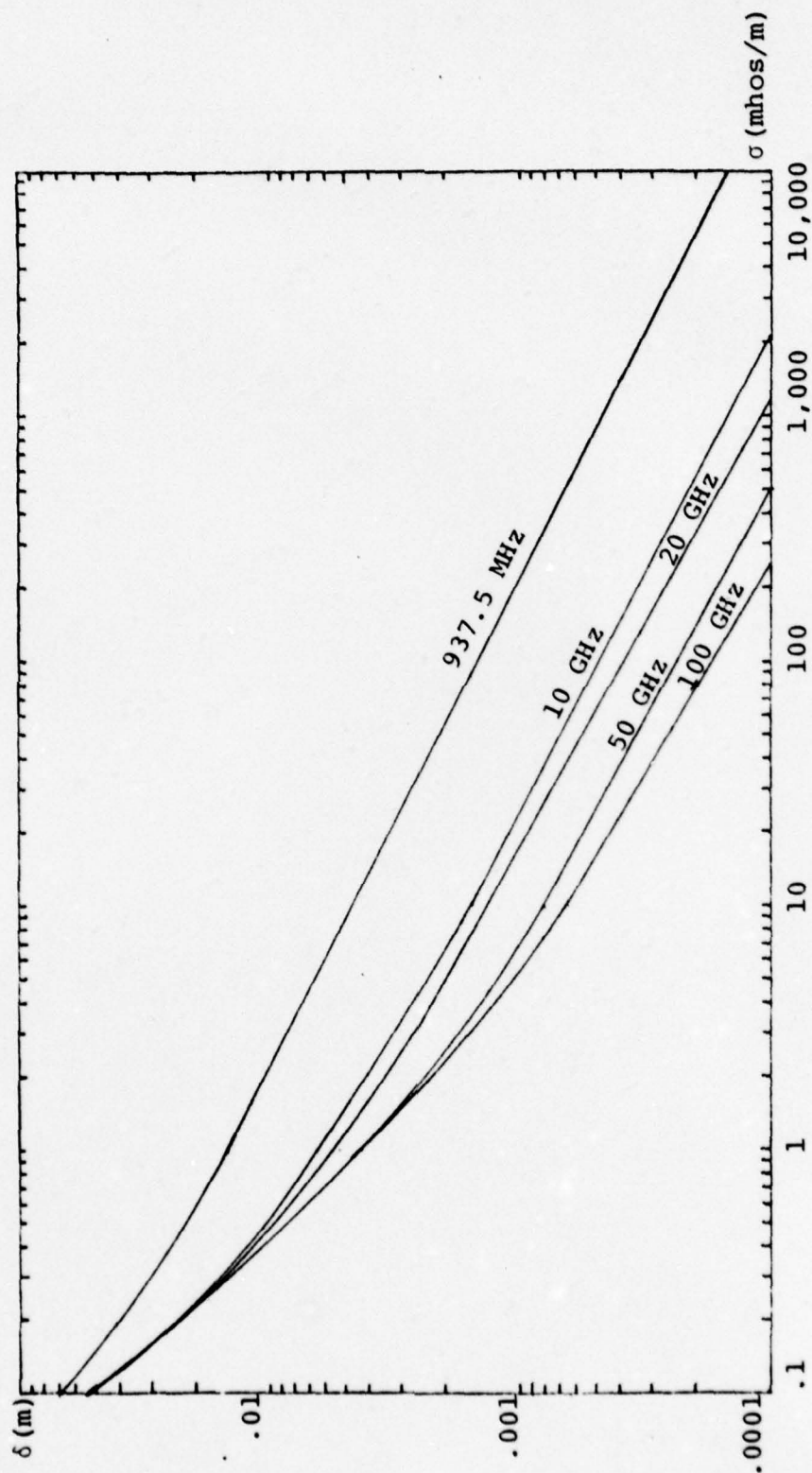


Figure 9. Graph showing relationship between frequency, conductivity, and skin depth.

The major effect of changes in frequency is in the required thickness, d . By specifying the frequency and the electrical conductivity, the skin depth, δ , and the thickness, d , also are specified. The relationship between frequency, electrical conductivity, and skin depth is shown in Figure 9.

By using Figures 8 and 9, a potential application of infrared current detection can be evaluated and the trade-offs between power levels, frequency, thickness, and thermal and electrical conductivities can be explored.

This trade-off, of course, is heavily influenced by the availability or existence of materials with an acceptable combination of thermal and electrical conductivities. Even the acceptable range has limitations due to practical considerations. For σ smaller than .1mho/m, σ and d are quite large even at high frequencies. At 100 GHz, $\sigma = .1\text{mho/m}$ yields $\delta = .05$ meters, and a thickness, d , of .1 meters. A coating 10cm thick is not practical in most applications. It can be seen from the curves in Figure 8 that large values of σ also are impractical because they require k to be less than .1, which is a thermal conductivity which very few materials have.

Materials with an electrical conductivity in a range of from one to ten mhos/m require thermal conductivities in an easily realizable range. There are not many materials in this range of electrical conductivities. Sea water, with a

conductivity of 5 mhos/m is a material in this electrical conductivity range. A list of other materials is given in Table 1. Unfortunately, very few of these materials are commonly occurring or easily produced on a large scale.

The lack of materials in the acceptable range of thermal and electrical conductivities does not necessarily indicate that this type of material is hard to produce. A more likely explanation for the scarcity of these materials is a lack of demand. Materials with low thermal conductivities are not normally used in applications where electrical conductivity is necessary or desirable. Materials with acceptable electrical conductivities ranging from one to ten mhos/m would be poor resistors, but much too conductive to be electrical insulators.

Table I. List of materials with thermal and electrical conductivities in the acceptable range of values for use as surface coatings in some frequency and power levels.

<u>Material</u>	$k, \frac{\text{Watts}}{\text{MOC}}$	$\frac{1}{\sigma}, \text{ ohms-meters}$	<u>Temperature</u>
1. Silicon Telluride	2.08	12.5	300°K
2. Thorium Oxide	3.47	4.0	300°K
3. Uranium Oxide	1.16	8	300°K
4. Zinc Oxide	7.8	50	300°K
5. Iron Titanate	See note 1	1	300°K
6. Sodium Silicate Glass	.82	100	300°K
7. Vanadate Glass	See note 2	100	300°K

Note 1: In the range of from 5 to 20 $\frac{\text{watts}}{\text{mOC}}$, exact data not available

Note 2: In the range of from .5 to 10 $\frac{\text{watts}}{\text{mOC}}$ exact data not available

IV. APPLICATIONS TO MORE COMPLEX SCATTERING
SURFACES OF NONMETALLIC MODELS

Even though the high-resistance surface preparations were not successful in providing a method of infrared current detection on metal surfaces, when applied to nonmetallic surfaces these surface preparations were quite successful in producing thermal profiles corresponding to the induced current distributions. The absence of the minus one reflection coefficient caused by the metal boundary eliminates the need for a minimum thickness of two skin depths. Since there is no reflected wave in the surface preparation to cancel the incident wave being transmitted the magnitudes of the net electromagnetic fields in the surface preparation are greater for a given thickness k than the fields which exist when there is a metal boundary present. Therefore the attenuation over a given depth d causes a greater energy absorption in the surface preparation on a nonmetallic surface.

The absence of the metallic surface has a beneficial effect on the thermal aspects of the problem also. The copper plate basically acted as a large heat sink, holding temperatures in the surface preparation very close to ambient temperature. When the copper boundary was removed, this temperature restriction was removed. The energy absorption in the surface preparation caused heating and tem-

perature increases throughout the material and at both boundaries. Thus the removal of the copper boundary increased the magnitude of energy absorption considerably and greatly increased the temperature increase caused by the energy absorbed.

Because of this, it was found that thermal conductivity was not critical, and an electrical conductivity of 100 to 160 mhos/m was sufficient to produce well defined thermal profiles for a very thin coat ($d = 2.7 \times 10^{-5} \text{m}$). The thermal contours produced accurately portrayed the current density magnitude measured in work by Wiedeman and Burton [6] on flat plates and by Burton, King and Blejer [7] on electrically long, electrically thick cylinders. These measurements were made by using probes in a very time consuming procedure.

A thickness of 2.7×10^{-5} meters was found to be satisfactory. Less thick coatings produced less heating, evidenced by fewer thermal profiles. Coatings thicker than 2.7×10^{-5} meters also produced less thermal detail. The thinner coatings produced unsatisfactory results because less energy was absorbed by the coating as most of the electromagnetic wave passed through it. As the thickness increases, more energy is absorbed by the coating and thus more heat generated. This trend continues up to the point where sufficient thickness exists for the exponential decay

$e^{-2z/\delta}$) to reach a very small magnitude. At this point more thickness does not mean substantially more energy absorption. Most of the incident energy is already being absorbed. At this point the volume of the coating, increasing at a constant rate, is increasing much more rapidly than the energy absorption rate. Thus the energy per unit volume, which affects the surface temperature, decreases drastically as the thickness increases. At this point more thickness does not increase surface temperature, but tends to decrease it, due to the thermal conductivity of the coating. The thermal conductivity of the coating tends to distribute the heat generated in the coating uniformly. Thus the tendency to uniformly distribute a constant amount of heat over an expanding volume yields less heat per unit volume. The magnitude of k determines the rate at which this distribution occurs, with higher thermal conductivities distributing the heat more quickly. If the heat is generated rapidly and the thermal conductivity is relatively low, the heat will not be distributed enough to prevent thermal profiles.

A. HALF WAVELENGTH SQUARE FLAT PLATE SCATTERERS

Infrared current detection techniques have been shown to be applicable to detection of induced currents in half wavelength square flat plastic plates. Selim and Burton [27] compared the results of irradiating five sheets of Teledel-

tos paper and showed that these results duplicated the measurements made by Wiedeman and Burton [6] using electrically small probes. This particular configuration was studied again in this report in order to compare the known results with the results obtained with resistive coatings other than Teledeltos paper.

The following half wavelength square flat plate scatterers were coated with various thicknesses of resistive coating, Television Tube Koat, manufactured by GC Electronics of Rockford Illinois. This coating has an electrical conductivity $\sigma = 160$ mho/m. The power level at the surface of the plate is 5mw/cm^2 . All plates were radiated with the incident wavefront arriving at 45° incidence, since this was a convenient laboratory arrangement and data was available to compare with the results. The distance from the plate to the radiating antenna was 3.5λ , sufficiently far to approximate the wavefront as plane.

1. Resistive Coating 6.18×10^{-5} Meters Thick

Good color contours were shown, but the coating was too thick and the sheet could not be heated to detectable levels in areas where current densities were known to be minimum due to the large volume over which the heat was distributed. The resulting isotherms are shown in Figure 10.

2. Resistive Coating 9.6×10^{-5} Meters Thick

Just as with the 6.18×10^{-5} meter thick coating, the

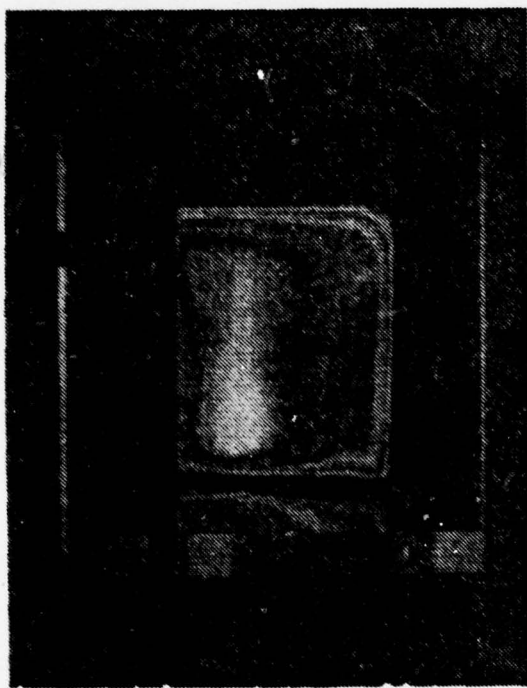


Figure 10. Half wavelength square plastic coated with 6.18×10^{-5} m of Television Tube Koat. Angle of incidence 45° . 20°C temperature window.

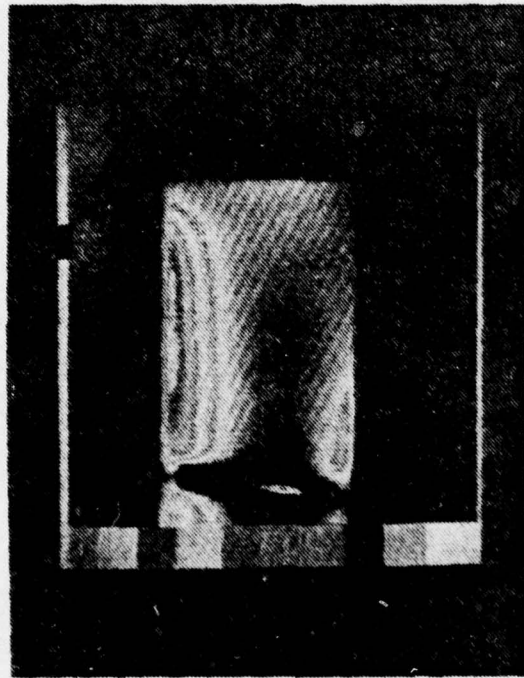


Figure 11. Half wavelength square plastic plate coated with $9.6 \times 10^{-5} \text{m}$ of Television Tube Koat. Angle of incidence 45° . 2° temperature window.

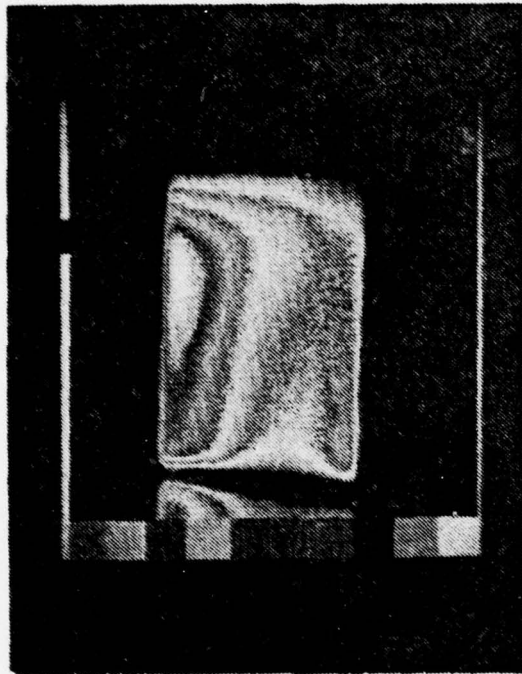


Figure 12. Half wavelength square plastic plate coated with $2.7 \times 10^{-5} \text{m}$ of Television Tube Koat. Angle of incidence 45° . 20° temperature window.

sheet could not be heated to detectable levels in areas where current densities were known to be minimum and still produce good isotherms in areas of greater current density. The tendency of the heat to be distributed throughout the volume prevented sufficient concentrations of heating necessary to produce isotherms. In Figure 11 this plate is shown with the camera bias adjusted so that minimum current density shows some temperature increase. With this bias adjustment the areas of high current density produce temperatures outside the temperature window, which appear white in the figure, and no current density distribution information is available in this area.

3. Resistive Coating 2.7×10^{-5} Meters Thick

It can be seen in Figure 12 that this thickness produced isotherms on the entire surface of the plate. The plate had no surface areas above or below the two degree temperature window. This display is entirely satisfactory for determining relative magnitudes of the induced current density throughout the plate and the isotherms also correspond exactly to the current distributions measured by Wiedeman and Burton [6].

B. OTHER AVAILABLE SURFACE COATINGS

Television Tube Coat, $\sigma = 160$ mhos/meter, was used for coating non-metallic scattering objects because it has an acceptable conductivity and is easy to apply, being packaged

in an aerosol container. It is a lacquer based aquadag coating, and was found to be unsatisfactory for use on some plastics because the propellant tended to dissolve the objects being sprayed.

There are many other brands of resistive coating that would be satisfactory in this application. The Duralac Chemical Corporation of Newark, New Jersey makes a lacquer based coating also, called Sea-Lac Chemical Coating. Micro-circuits Company of New Buffalo, Michigan manufactures resistive coatings with a wide range of available resistances. Acheson Colloids Company of Port Huron, Michigan produces a water based Aquadag coating.

However, none of these products are marketed in an aerosol applicator, and the lack of equipment necessary for spraying these coatings onto the surfaces being examined made it impossible to test these preparations on scattering objects. The coating must be applied uniformly; without spraying this could not be done in the laboratory.

C. ELECTRICALLY THICK, ELECTRICALLY LONG CONDUCTING CYLINDERS

Electrically long and electrically thick conducting cylinders are of interest as scattering objects in an electromagnetic field. Such a cylinder is a close approximation to the shape of rocket fuselage, and a simple first order approximation of the fuselage of aircraft. The charges and

currents induced by an electromagnetic field incident on the cylinder (or aircraft) are of concern in developing shielding to protect sensitive electronic systems.

Theoretical and experimental work has been done for thick cylinders by Burton, King, and Blejer [7]. Theoretical and experimental data has been reported for cylinders with heights, h , such that $kh = 3.5\pi$ and radii a such that $ka=1$ where $k=2\pi/\lambda$. For $f=937.5\text{MHz}$, $\lambda=32\text{cm}$, $a=5.1\text{cm}$ and $h=.56\text{m}$.

For observations of these cylinders a plastic pipe of proper dimensions such that $ka=1$ and $kh=3.5\pi$ for $f=937.5\text{ MHz}$ was sprayed with Television Tube Koat, $\sigma=160\text{ mho/meter}$. The coating was applied with a thickness of $4.2 \times 10^{-5}\text{m}$.

Due to the height of the cylinder relative to the wavelength, the spherical wavefront could not be approximated as plane. The incident power at the top and the bottom of the cylinder varied by over 2mw/cm^2 when the antenna was less than four wavelengths from the scattering object. It was found that when the antenna and the cylinder were separated by eight wavelengths the field strength at the top and bottom of the cylinder was approximately equal, at 2mw/cm^2 . For this reason, an eight wavelength separation between the antenna and cylinder was used for experiments using infrared current detection techniques.

Measurements of induced current magnitude made by Burton, King, and Blejer [7] were used as a comparison for the results obtained by the infrared current detection method.

A graph of these results is given in Figure 13. The infrared current measurement technique was applied to the previously described cylinder coated with Television Tube Koat, using a frequency of 937.5MHz. Due to limitations imposed by the size of the laboratory, the cylinder could only be viewed with the infrared camera for angles of $\theta=80^{\circ}$, 100° , 120° , 140° , and 180° , where θ is the angle measured from the point on the cylinder opposite the point where the incident wave was normal to the cylinder to the point where the cylinder was being viewed. Photographs of the isotherms that were observed at the different angles are shown in Figures 14 through 18.

A comparison of Figure 13 with Figures 14 through 18 show that the infrared current detection method produces results almost identical to the data collected using the probe method. The only area where differences are noted is at the top of the cylinder and this is due to the irregularity of the top edge of the cylinder.

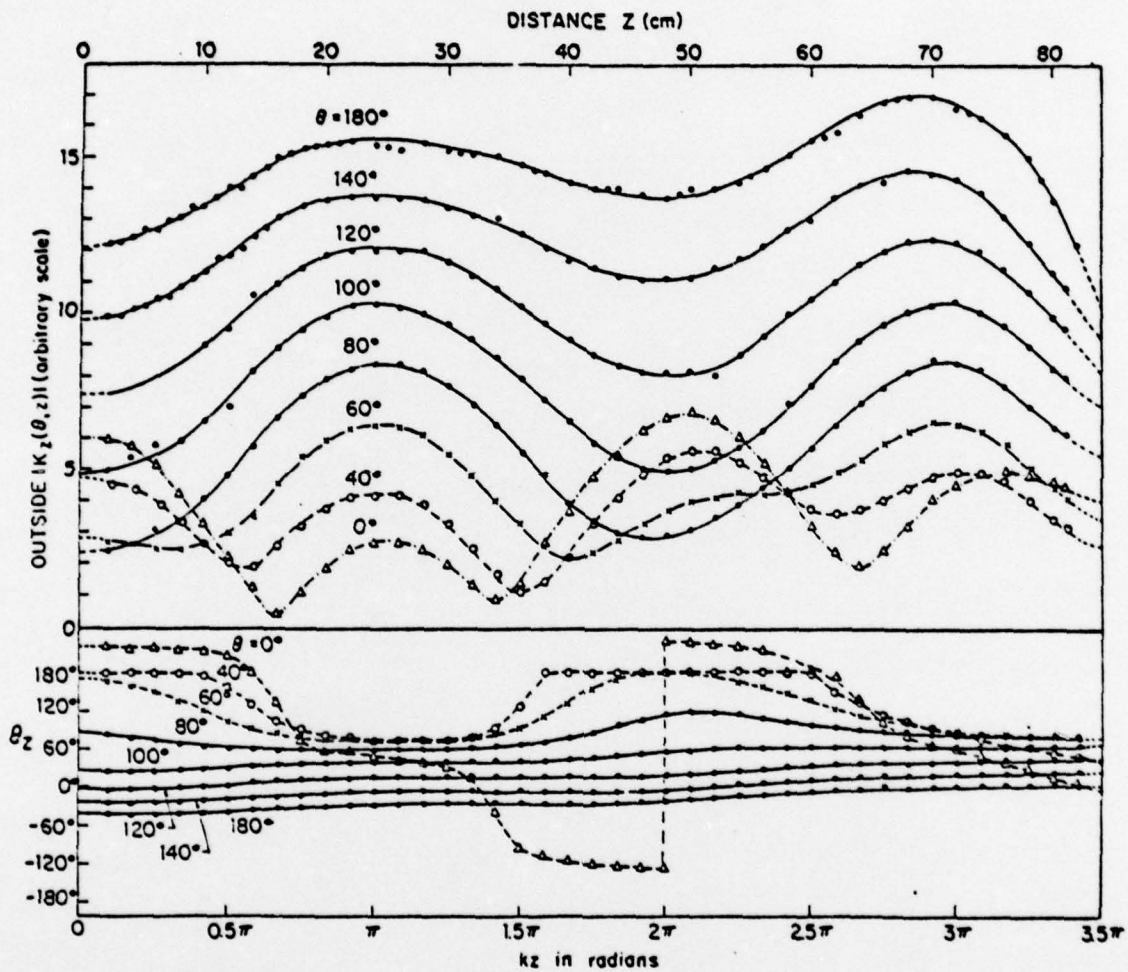


Figure 13. Measured magnitude and phase of surface density of outside axial current on tubular cylinder. E-polarization; $kh=3.5\pi$, $ka=1$, $\lambda=48.0\text{cm}$. [7]

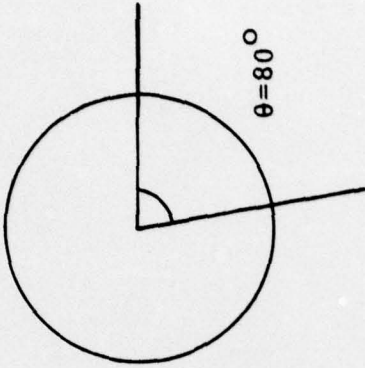
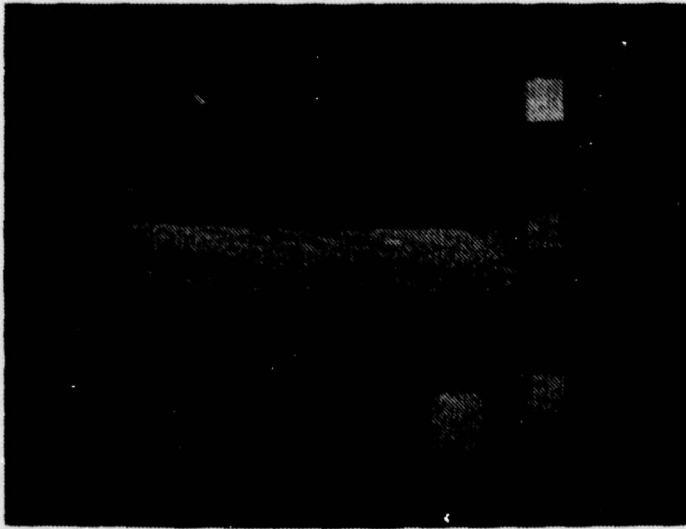


Figure 14. Electrically thick, electrically long conducting cylinder viewed at $\theta = 80^\circ$. Temperature window is 10C.

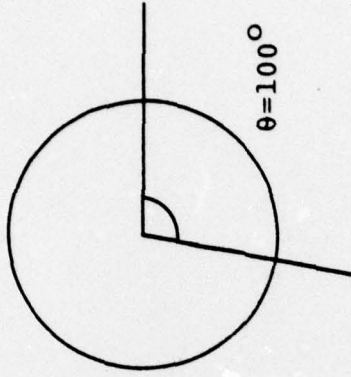


Figure 15. Electrically thick, electrically long conducting cylinder viewed at $\theta=100^\circ$. Temperature window is 10C.

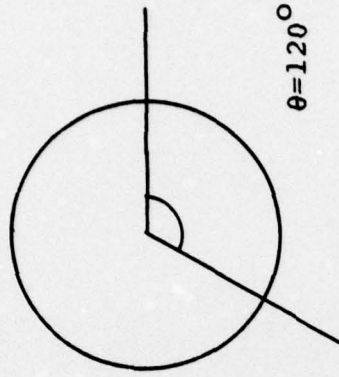
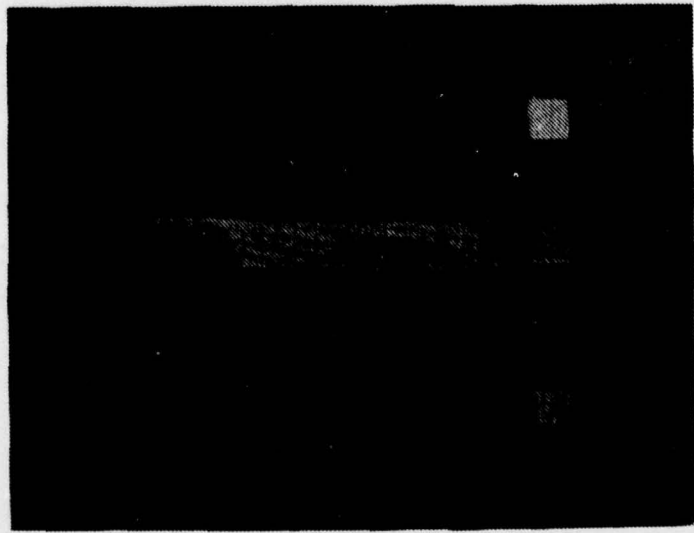


Figure 16. Electrically thick, electrically long conducting cylinder viewed at $\theta = 120^\circ$. Temperature window is 10C.

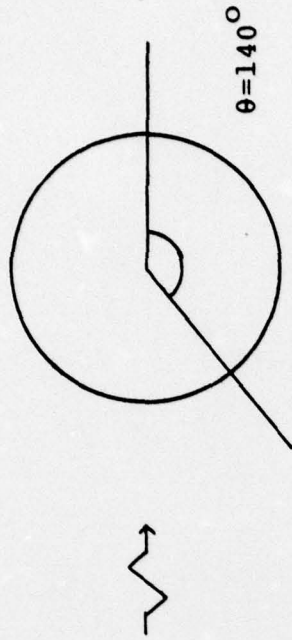
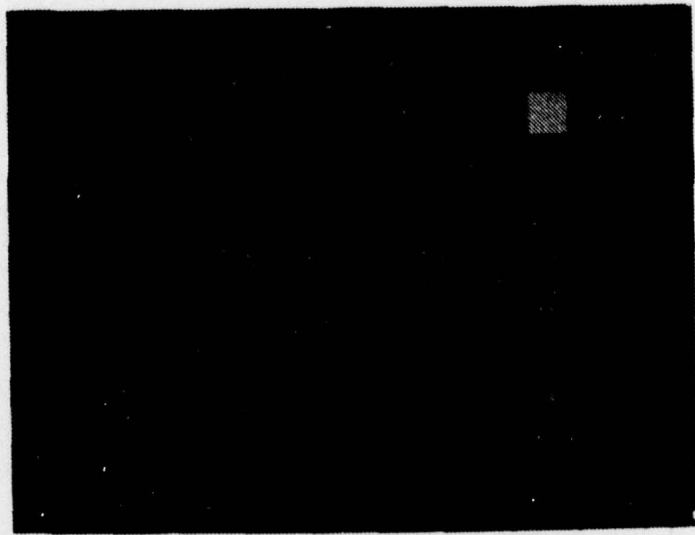


Figure 17. Electrically thick, electrically long conducting cylinder viewed at $\theta=140^\circ$. Temperature window is 10C.

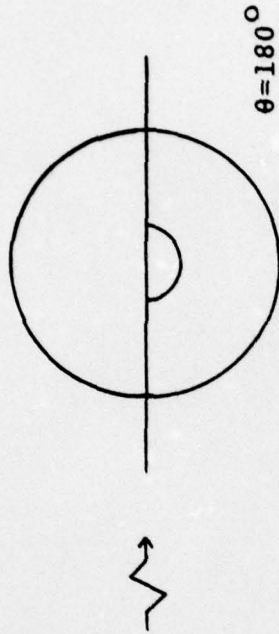
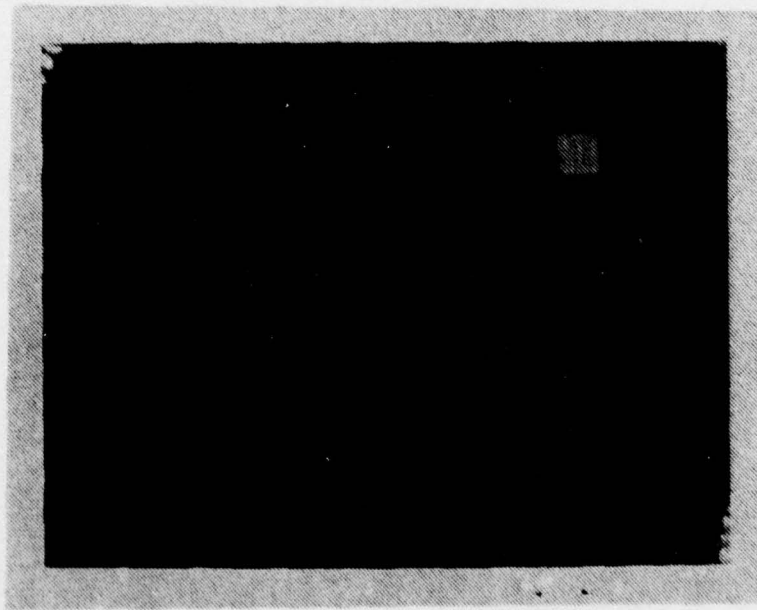


Figure 18. Electrically thick, electrically long conducting cylinder viewed at $\theta = 1.80^\circ$. Temperature window is 1 C.

V. CONCLUSIONS

Infrared detection methods can accurately determine magnitudes of surface current distributions on scattering objects if the surface is properly prepared to enhance infrared emissivity and the amount of heat generated. All scattering objects studied (flat plates, thin cylinders and thick cylinders) using infrared imaging have yielded results that completely agree with the known current distributions for objects of those shapes if the surface was properly coated.

In order for this procedure to evolve from its basic laboratory orientation to a practical procedure for use in the field, satisfactory surface preparations must be found. These preparations must be satisfactory in the sense that they are easily manufactured, easily applied to the surface in uniform thickness, and possess parameters which permit their use in small thicknesses and with moderate power levels.

More work is needed in comparing results obtained by infrared measurements with known results. If there are shapes, sizes, frequencies, or power levels which do not yield accurate results, these should be identified and examined.

More work is needed also in the area of interpretation of the infrared images. A method of translating surface temperature changes to values of current density is needed. A temperature reference needs to be included in the infrared display.

None of the above mentioned problems seems insurmountable, and the advantage to be gained by solving them are impressive. Real-time results are available. The technique is simple and fast, and the time-saving that can be realized by employing infrared current detection methods is great.

BIBLIOGRAPHY

1. La Varre, C. A., and Burton, R. W., "Thermographic Imaging of Electromagnetic Fields", Thesis Report NPS-52ZN75121, Naval Postgraduate School, Monterey, California, December, 1975.
2. Selim, J. D., and Burton, R. W., "Infrared Detection of Surface Charge and Current Distributions", Thesis Report NPS-62-77-001, Naval Postgraduate School, Monterey, California, December, 1977.
3. Hayes Aircraft Corporation, An Introduction to the Principles of Infrared Physics, p. 71, 1958.
4. Özisik, M. N., Radiative Transfer and Interaction with Conduction and Convection, p. 69-74, 100-104, Wiley, 1973.
5. Bramson, M. A., Infrared Radiation, p. 127, Plenum Press, 1968.
6. Burton, R. W., Private communication.
7. Burton, R. W., King, R. W. P., and Blejer, D. J., "Surface Currents and Charges on an Electrically Thick and Long Conducting Tube in E- and H- Polarized, Normally Incident, Plane-wave Fields", Radio Science, v13 nr.1, p. 75-91, January-February 1978.

INITIAL DISTRIBUTION LIST

	No. Copies
1. Defense Documentation Center Cameron Station Alexandria, Virginia 22314	2
2. Library, Code 0142 Naval Postgraduate School Monterey, California 93940	2
3. Department Chairman, Code 62 Department of Electrical Engineering Naval Postgraduate School Monterey, California 93940	1
4. Professor R. W. Burton Department of Electrical Engineering United States Air Force Academy Colorado 80840	10
5. Lieutenant William David Russell, USN Route 4 Gardner Road Stockbridge, Georgia 30281	2
6. Mr. Jacob Scherer Post-Doctoral Program RADC-RBC Griffiss AFB, New York 13441	2
7. Professor Glen Smith School of Electrical Engineering Georgia Institute of Technology Atlanta, Georgia 30332	1
8. Professor Lamar Allen University of South Florida Electrical and Electronic Systems Tampa, Florida 33620	1
9. Professor Robert Catellessa Clarkson College of Technology Potsdam, New York 13676	1
10. Dr. W. Everett SCEE Cherwood-Oneida Lake Walnut Grove Bridgeport, New York 13030	1

11. Mr. Warren Peele 1
Electrical Engineering Department
Purdue University
West LaFayette, Indiana 47907
12. Dr. C. E. Baum 1
AFWL/EL
Kirtland AFB
Albuquerque, New Mexico 87118
13. Mr. P. Castillo 1
AFWL/ELE
Kirtland AFB
Albuquerque, New Mexico 87118
14. Professor K. Iizuka 1
Department of Electrical Engineering
University of Toronto
Toronto, Canada
15. Dr. Robert Mailloux 1
Electronics Technology Division/RADC
Hanscom AFB, Massachusetts 01731
16. Professor Walter H. Ku 1.
Department of Electrical Engineering
Cornell University
Ithica, New York 14850